Final Report

For

Electron Spectrometer for ATS I and II

(March, 1965 – December, 1967)

Contract No: NAS5-9542

COSMIC RAY GROUP

School of Physics and Astronomy

UNIVERSITY OF MINNESOTA

Final Report

For

Electron Spectrometer for ATS I and II

(March, 1965 - December, 1967)

Contract No: NAS5 - 9542

Goddard Space Flight Center

Contracting Officer: E. K. Cockerham

Technical Monitor : Forest H. Wainscott II

Prepared by

School of Physics and Astronomy

University of Minnesota

Minneapolis, Minnesota

Project Manager: John R. Winckler

For

Goddard Space Flight Center

Greenbelt, Maryland

Final Report

For

Electron Spectrometer for ATS I and II

(March, 1965 – December, 1967)

Contract No: NAS5-9542

Prepared by

School of Physics and Astronomy

University of Minnesota

Minneapolis, Minnesota

For

Goddard Space Flight Center

Greenbelt, Maryland

ABSTRACT

This report summarizes a measurement at synchronous orbit of energetic electrons detected by a magnetic deflection spectrometer at energies between 40 keV and 1 meV for the purpose of investigating the origin of these energetic electrons in the trapped radiation. The report includes a brief introduction covering the ATS-1 mission, the data tapes received and some pertinent facts about the operation. A brief discussion of the trapped radiation is given and the specific objectives of the experiment namely, to investigate the acceleration mechanisms during magnetic storms and to perform exploratory measurements in the outer zone, are outlined. The advantages of the geostationary orbit for these purposes are described. A rather detailed description of the construction and operation of the experiments follows, including the reduction of data and the determination of electron fluxes in space. Different types of data plots and outputs and the problem of noise filtering are described. A list of titles and abstracts of key published papers is given, followed by a detailed summary of the principal results, their meaning, and theoretical interpretation. This latter section includes comparisons with the OGO electron spectrometer, which permits simultaneous measurements at several places in the magnetosphere. The magnetospheric substorm is identified as a primary mode of injection of electrons into the outer radiation belts.

LIST OF ILLUSTRATIONS

TABLE OF CONTENTS

Introduction

A brief summary is presented here of experiments constructed, flown and analyzed in connection with the geostationary orbit satellite ATS-I and the gravity gradient test satellite, ATS-II. The School of Physics, University of Minnesota, designed an electron spectrometer for the measurement of electrons occurring in the trapped radiation regions between energies of 50 keV and 1 meV. These instruments utilized magnetic deflection coupled with scintillation detectors for the electrons. Details of the experiment in addition to those included herein, are contained in our quarterly progress reports and in published papers referenced herein and listed in the Bibliography. The necessary thermal-mechanical and prototype models were delivered as well as a final flight model of the experiment which was placed in orbit December 7, 1966. The experiment continued to function until January 1968, when the highest energy channel stopped working. In June of 1968, the other two channels ceased to operate and the experiment was concluded. Thus, approximately one year (counting some data gaps) of equivalent full-time data was obtained with very high time resolution and also with good directional and energy discrimination for the lower energies. This time compares favorably with the one year estimated life based on a predicted 50% failure probability.

Failure analysis has not made the failure difficulty clear. The failure mode can in certain respects be duplicated in the laboratory by changing the power supply voltage levels so that this explanation,which lies outside of the University of Minnesota package,remains a possibility. During construction and test of the unit, some difficulties were encountered with field effect transistors. The failure mode caused by these field effects, however, does not duplicate that observed in space. The exact difficulty, thus, does not seem at this time to be apparent.

Approximately 600 data tapes have been obtained from the ATS program office covering the above period. Data reduction has been laborious for many reasons because of the high density packed tape format, the necessity to change at Minnesota from the CDC 3600 computer to the University of Minnesota 6600 computer, and the necessity of elaborate filtering routines for removing spurious counts injected by telemetry noise originating in the ATS EME telemetry circuit.

The geostationary orbit is exceptional for its position in the outer Van Allen radiation belt and because of the geostationary nature of the satellite in the geomagnetic field. Thus, a completely new view of the particle variations and important clues to the origin of the trapped radiation have been obtained. Extensive use has been made of the vector magnetic field also measured on board the ATS-I mission. After December, 1967, the data analysis was supported under grant NGL-24-005-008 from NASA Headquarters and work is continuing, funded by that source.

An identical copy of the experiment was launched on the ATS-II mission in April, 1967. Unfortunately, the satellite failed to inject into the desired orbit and was not stabilized although some data was obtained from April 1967 through October 1967. The lack of aspect information made the analysis so difficult that no effort has been expended in this direction. It was determined, however, that the experiment was operating satisfactorily during the above period. Data tapes from the ATS-II mission are on hand but computer programs for cracking the packed digital format are available only for the CDC 3600 computer. For certain exceptional periods it may be possible to make use of the ATS-II simultaneously with ATS-I in a manner similar to the comparison of ATS-I with the OGO-III satellite. At present we have not begun any such effort.

Objectives

Before one can begin to understand the purpose of the Minnesota experiment on ATS-I and II, he must be a little familiar with the characteristics of the environment in which the experiment operated.

In addition to gravitational field, the earth possesses a magnetic field. The axis of this field is displaced very slightly from the geographic center of the earth and is inclined to the earth's polar axis at an angle of approximately 11°. The overall shape of the magnetic field is that of a distorted dipole. Within the earth's magnetic field exist the Van Allen radiation belts. These belts consist of protons and electrons which are "trapped" within the field. The electron component was studied on ATS.

These trapped electrons exhibit interesting types of motion within the trapping regions. The electrons spiral along a field line in a northerly or southerly direction, and, as they get closer and closer to the earth, the magnetic field becomes stronger and stronger. When the field becomes strong enough, the electrons stop their forward motion (point M. Figure 1) and reverse their direction of travel. In this way an electron "bounces," and subsequently rebounds in the opposite direction. This phenomenon is exhibited in both hemispheres as the particles approach the surface of the earth, and hence they are "trapped," continually bouncing on a magnetic field line between the northern and southern hemispheres.

In addition to the electron's bouncing motion, it should be mentioned that they slowly drift around the earth in an easterly direction. (The term "slowly" refers to a comparison with the bounce time of the electron: the time required for one to bounce in the northern hemisphere, travel down to the southern hemisphere, bounce, and return to the starting point is of the order of a second; they gradually drift around the earth with a period on the order of an hour or so.)

The principal scientific purpose of the ATS experiments is to understand the origin of the energetic electrons trapped in the magnetosphere. It is well known that electrons of 40 keV energy and higher are not present in sufficient numbers or at the right time in the interplanetary space to account for the high intensity of these electrons in the trapped regions, thus one must look for the acceleration mechanism in the magnetosphere itself. The problem may be posed in a number of questions to which these experiments may contribute answers.

1. Since these electrons appear in conjunction with magnetic storms, what are the particular magnetic storm mechanisms which can be associated with the electron acceleration?

2. What is the association between effects seen at large distances from the earth in the equatorial plane on the trapped electrons and the precipitation of these electrons into the atmosphere in association with the aurora?

3. What is the detailed time structure of the variations seen at synchronous orbit down to several Hz and are these associated with the pulsations found in magnetic pulsations, aurora and x-ray measurements at ground level?

Information on the trapped electrons during magnetic storms has been available from many satellite missions. (See for example, Hess, 1968). These observations, in most cases, give information about the presence of trapped particles with no definite indication as to the mechanisms of acceleration or injection into the radiation belts. It is the purpose of the present experiments to make a significant step in this direction by providing answers to the above questions, (questions which can be formulated in advance) and at the same time, be exploring a new and interesting region of the magnetosphere and to discover new and unknown relations between the presence of trapped particles and other variations observed.

There were two major adavantages with the ATS geostationary orbit:

(1) Since the earth's magnetic field lines rotate with the earth, and the particles in general bounce along a field line, the experiment will be exposed primarily to time variations (as opposed to spatial variations) in the electron population of the belts, since the satellite also rotates with and stays on the same field line (and hence stays with the same particles on that field line and can examine how their characteristics change with time). (Other non-geostationary satellites move through the magnetic field as time passes, and the changes in trapped particle distributions they witness cannot be said to be definitely a time variation or a spatial variation, but only a combination of both; hence one can't really tell whether the changes he has measured are due to motion of the satellite to a different point with respect to the particles originally near it, or because the last measurement was made at a different time than the preceding one.)

(2) The second desirable feature is that while the satellite is in orbit, balloons and rockets may be launched at the point where the field line, that the satellite is on, intersects the earth (point X, Figure 1). Since the same electrons stay on the same field line (recall this is an approximation) measurements made by the balloon can be correlated with measurements made on the satellite over long periods of time. When the balloon instruments detect some of the electrons on the field line striking the atmosphere, the satellite can tell simultaneously what is happening to the electrons in space, and perhaps indicate why some are changing their mirror points and being lost in the atmosphere.

I. Experiment Operation

A. Spectrometer Description

The University of Minnesota electron spectrometers on board the ATS-I and ATS-II satellites are magnetic deflection charged-particle momentum analyzers. They are sensitive only to electrons and measure the spectral distribution summed within three energy ranges, 50-150 keV, 150-500 keV, and 500-1000 keV.

The basic components of the spectrometer are illustrated in Figure 2. A particle collimator is attached to the entrance of the electromagnet and allows into the magnet only those particles whose velocity vectors lie directionally within a "cone" of about 7° half-angle. (The actual cross section of the entrance aperture is a square.) The particles passing through the collimator opening then enter the magnetic field region, and their trajectories are bent according to their velocities, their charge-to-mass ratios, and the strength of the magnetic field. The only (non-zero) magnetic fields generated between the pole faces are such that only electrons in the three previously mentioned energy ranges can possess straight-line trajectories from the exit region of the magnetic field (Point C) toward the plastic scintillator (Point D). The magnet pole face has an overall wedge-shape because this particular shape generates magnetic fringing fields which produce both vertical and horizontal focusing, and also the particular choice of angle between the two sides of the wedge (the sides located at Points B and C) allows particles in the wings of a particular energy range to strike the scintillator as well as those in the center of the energy range, regardless of from what direction in the entrant cone of angles they come. (The ATS spectrometers are similar in some respects to the electron spectrometers flown on the OGO I and OGO III satellites by the University of Minnesota. The ATS spectrometers,

however, are smaller, require less power, and examine a smaller range of electron energies. The OGO spectrometers are discussed by Kane, Pfitzer, and Winckler (Sept., 1966).

The magnetic field is periodically stepped through four different field values, remaining at each level for forty milliseconds, and completing one cycle of all four values within 160 milliseconds. (The field strengths attained are approximately 0 gauss, 460 gauss, 900 gauss, and 1720 gauss.) The zero field magnet step is included so that during that time we may determine a background correction for the data.

The detector consists of an NE102 plastic scintillator, a lead glass light pipe, and a photomultiplier tube (Amperex XP1110). The plastic scintillator and the lead glass light pipe are enclosed in a tungsten shield. Shielding is maintained in all directions with respect to the scintillator such that there is a minimal amount of shielding of 10 gm/cm^2 for virtually all straight line paths from the scintillator to the outside of the experiment package. The most important source of background counts in the spectrometer is the bremsstrahlung x-ray photons generated when the Van Allen belt electrons strike the surfaces of the spacecraft and its experiment packages. For this reason, the shielding used is all high-Z material (tungsten and lead) which has relatively large absorption coefficients for these background photons. Also for this reason the scintillating material chosen was plastic, NE102, as opposed to higher-Z material (such as sodium-iodide) which is more efficient for detecting x-ray photons. The shielding scheme for the ATS spectrometers appears to be adequate, for on ATS-II the background counting rate in the low energy range is rarely more than 5% of the total counting rate, and in the middle and high energy ranges it is rarely more than 3-4% of the total count rate. The background contribution to the total count rate is known accurately enough so that the 15-minute corrected averages have an error less than 1%, and for the low and middle energy ranges it is typically about 0.3%.

All surfaces of the scintillator (except the one at the interface of the lead glass and plastic scintillator) were coated with a very thin reflective-aluminum layer. An entrance window to the scintillator for the electrons properly bent by the magnet is provided at point D in Figure 1. A section of light-tight quarter-mil mylar film is placed over this surface of the scintillator to insure the light-tightness of the detector system.

The pulses generated by the photomultiplier are fed into what is in essence a three-channel pulse height analyzer, each channel calibrated to accept pulses produced by electrons in only one of the three energy ranges previously mentioned. Background pulses accumulated when the magnet is in the zero gauss step are accumulated in three separate spacecraft accumulators. The number of pulses generated in each of the three energy ranges is stored in each of three experiment scaler circuits as digital information. (These scalers each have a capacity of 2^{10}.) Every 160 milliseconds counts are accumulated in each of the three energy ranges for a period of 40 milliseconds and telemetered to a ground tracking station. The background information is telemetered once every 5.12 seconds.

The data sampling schedule is synchronized with the telemetry sequence of the satellite. (Please refer to Figure 3.)

At some arbitrary time, t=0, both the telemetry and the magnet begin a cycle. The magnet remains in each of four successive basic steps for a period of 40 milliseconds. During this period, counts are accumulated and stored in either the appropriate experiment scaler circuit or spacecraft background accumulator, depending on which part of the magnet cycle we are considering.

At time t=0 the magnet is in the zero gauss step, and the pulse height analyzer is set to allow counts in the 150-500 keV range into the appropriate background accumulator. This magnet step is denoted BGβ since

background ("BG") data is accumulated during this step, and it is data pertaining to the second energy interval 150-500 keV (denoted as channel beta). At time t=40 milliseconds the magnet current increases and the magnetic field is now maintained at 460 gauss, and during the next 40 milliseconds all counts corresponding to energies 50-150 keV are stored in the scaler circuit for that energy channel (denoted as channel alpha). This magnet step is denoted as step alpha for obvious reasons.

At t=80 milliseconds the magnetic field increases to 900 gauss, and all photomultiplier pulses corresponding to energies of 150-500 keV particles are stored in the scaler circuit for this energy channel (denoted as channel beta). This magnet step is denoted as step beta.

Finally at t=120 milliseconds, the magnetic field increases to 1720 gauss, and all pulses corresponding to electrons of energy 500-1000 keV are stored in the third scaler circuit for this third energy range (denoted as channel gamma). This magnet step is denoted as step gamma.

The magnetic field begins another cycle at t=160 milliseconds. However, from t=160 to t=200 milliseconds, background data is now collected for channel gamma. Also, from t=320 to t=360 milliseconds, background data is collected for channel alpha (at the start of the third magnet cycle). This data gathering cycle is then complete and continues to repeat. The sequence of data gathering from the time t=0 is then the following:

$$BG\beta,\alpha,\beta,\gamma,BG\gamma,\alpha,\beta,\gamma,BG\alpha,\alpha,\beta,\gamma,BG\beta,\alpha,\beta,\gamma,....$$

where the system dwells in each state for 40 milliseconds.

Thus, data is gathered in each of the three energy intervals for 40 milliseconds once every 160 milliseconds, and background information is accumulated for a total of 400 milliseconds every 5.12 seconds in each energy interval. The data is telemetered back to the tracking station in such a manner that the above time resolution is preserved. (Note: A command can

be issued to the experiment such that the magnetic field remains at zero gauss, and in this mode background data can be gathered for 40 milliseconds every 160 milliseconds in each energy channel.) It should be noted that the number of background counts in each spacecraft accumulator is telemetered as digital information; the number of counts in each scaler circuit, however, is converted by the experiment from digital to analog information before subsequent telemetry to the tracking station.

B. Calibration of the Spectrometer

a. Magnet Current and Edge Setting

The proper choice of the magnetic fields to be used was made in the following manner. A calibrated solid state detector system was placed in the proper positions at the exit of the electromagnet so as to determine the maximum and minimum energies of the particles leaving the magnet as a function of DC magnet current. (A strontium-90 source placed in the collimating slit was used as a source of electrons over the three energy ranges.) The magnet current was adjusted until the range of energies allowed by the magnet was that which we wished to study (i.e., 50-150, 150-500, and/or 500-1000 keV), and this was the current value chosen for that particular magnet step. (The pole face was designed such that the desired three energy ranges were approximately attainable with three proper choices of magnet current.)

The electronic edges of the three-channel pulse height analyzer were set in the following manner. The lower edge of the 50-150 keV window was adjusted downward until the tube noise above this lower edge began to become appreciable. The upper edge of this window and the lower edge of the middle (150-500 keV) window were set approximately using the conversion electrons of Co^{57}. (The setting of these particular edges is not too critical an adjustment, since the resolution of the detector in the low

energy region is quite poor anyway, and the magnet is the primary selector of the energies observed.) The 500 and 1000 keV edges were set using the conversion lines of Bi^{207}. (All sources were placed directly on the face of the scintillator; the magnet was not used at all in the setting of these electronic edges.)

b. Determination of Flux Calibration

The following is a discussion of the procedure used to convert the counts/sample number produced by the experiment to an actual estimate of the flux of electrons being measured.

During the spacecraft thermal-vacuum test a few months prior to launch, a special strontium-90 source was placed at the entrance aperture of the experiment. This source was placed flush with the outermost collimator opening; the active area of the source was larger than this opening and indeed filled the entire field of view. The average counts per sample in each of the three energy intervals was then recorded and corrected for background.

The absolute spectrum of the same strontium-90 source was then measured in a vacuum chamber at the University of Minnesota over a small cone in the forward direction from the source. It was assumed that the source was isotropic over a small cone in the forward direction, the cone of entrant directions allowed by the spectrometer. From the measurement of the absolute spectrum of the source, its equivalent strength as an isotropic emitter in the forward direction is known, j(E) electrons/cm^2-sec-ster-keV (where E denotes an energy dependence). The function j(E) is then averaged with respect to energy E over the ranges 50-150 keV, 150-500 keV, and 500-1000 keV to obtain the average differential spectrum of the source in each of the three spectrometer energy ranges, denoted as

$$\bar{J}_\alpha \text{ , } \bar{J}_\beta \text{, and } \bar{J}_\gamma$$

Since the average counts/sample in each of the three energy intervals is known for this particular source (denote them $N(\alpha)$, $N(\beta)$, $N(\gamma)$, then the constant of proportionality between the two numbers may be determined for each channel:

$$\bar{J}_i = K_i N(i), \quad i=\alpha,\beta,\gamma$$

Thus K_i may be determined for each channel, and used as a constant to compute the first-order spectrum necessary to produce a certain set of (observed) count rates. (To compute a more accurate second order spectrum it is necessary to iterate the above computation taking into account the spectral dependence of K_i.)

The preliminary values of the constants K_i have been determined for the ATS-II spectrometer and are listed below (K_i has the following units: (electrons/cm^2-sec-ster-keV)/(count/sample)):

$$K_\alpha = 4.50 \times 10^2$$
$$K_\beta = 7.79 \times 10^1$$
$$K_\gamma = 4.03 \times 10^1$$

Thus a count rate of 100 counts/sample in channel alpha would imply the flux producing this count rate is approximately 4.50×10^4 electrons/cm^2-sec-ster-keV in the range 50-150 keV.

C. Data Analysis

a. Routine Data Analysis

All experimenters data tapes received by the University of Minnesota underwent a routine data analysis. This procedure formed 15-minute averages of the background-corrected count rates in each of the three spectrometer channels and utilized all "good" data (i.e., data that was not bad or padded and which was taken at times when other spectrometer parameters indicate the instrument is functioning properly). These averages were calculated and tabulated at the University of Minnesota Numerical Analysis Center by

a CDC (Control Data Corporation) 6600 computer. Also computed and tabulated was information pertaining to the quality of the data analyzed. (Such items as percent bad data encountered, percent padded date encountered, number of points summed to form the averages, background rates, error in corrected rates and background rates, temperature of the experiment, etc. were all computed and tabulated to indicate the quality and significance of a particular 15-minute average of the three corrected count rates.)

As the fifteen minute average changes were plotted it was discovered that during the period in which the telemetry data was recorded by certain ground stations, the count rates, especially in low count rate channels, became highly distorted. Further investigation showed that the use of lower gain receiving antennas resulted in noise injection into the telemetry signal which created spurious frequencies in the PFM system. It was thus necessary to devise elaborate filtering routines to remove the spurious intervals. This was accomplished by providing an automatic bin-sort in which the count rates were stored in a series of discreet ranges in 25 second samples. These bin-sort profiles were normally narrow Gaussian distributions. During noisy periods, however, counts appeared in bins far in the wings of the Gaussian. After examination of the character of the noise in this manner, certain routines were devised to correct the data and recalculate the corrected averages. It has been found necessary to pass all ATS data from the electron spectrometer through such a filtering routine. This results in almost complete elimination of the noise problem. It has been achieved at considerable cost in time, effort and programing expense.

The 15-minute average count rates are also routinely converted to fluxes to form a first-order spectrum. These flux values are then fitted with both a least-squares exponential curved and a least-squares power law curve.

These two curves are of the form

$$j(E) = C_s \exp(-E/E_o)$$

and

$$j(E) = C_1 E^{-K}$$

where E denotes energy of the electrons, E_o is the exponential folding-energy (determined by the least-squares fit), and C_s is a constant (also determined by the least-squares fit). C_1 and K are constants determined by the least-squares power law fit. In both instances j(E) is the differential electron flux and has the units of electrons/cm^2-sec-ster-keV. The energy E is in units of keV. Iteration may or may not be used in determining the averaged flux values over the three energy intervals sampled by the experiment, and this will generally be indicated whenever this data is presented. The results of the routine data analysis procedures are listed in tabular form. These results include the fifteen minute averages (and errors) of the counts/sample number for each of the three energy intervals, the first order estimates of the differential fluxes in the three energy ranges, and the constants C_s, E_o, C_1, and k.

b. Non-routine Data Analysis

Non-routine data analysis procedures are by definition those analysis procedures that are not applied to all data received. The special analysis procedures which were employed are described briefly below.

(1) Pitch Angle Distributions: By utilizing the data on the ephemeris tapes (magnetic field models), it is possible to generate a pitch angle distribution of the electrons using maximum time-resolution data. (Correlation of our data with that gathered by Coleman, et al. with their magnetometer on board ATS-II produced some meaningful pitch angle distributions which were free from uncertainties imposed by using a model of the magnetic field.)

(2) Spectral Analysis Distributions: The sampling of the spectrometer is frequent enough such that periodic fluctuations in the electron spectrum can be determined for virtually all frequencies less than 3.12 cycles/sec. It should be pointed out that the bounce times of low energy electrons (50-150 keV) in the vicinity of the satellite should be in the frequency range amenable to analysis. (The longitudinal drift period of electrons in this energy range is considerably longer (on the order of 10^2 minutes) and is in the range of frequencies accessible to spectral analysis procedures.)

(3) Correlation with Balloon Data: The University of Minnesota was involved in a program to launch balloons to the top of the atmosphere in the region where the field lines in the vicinity of the ATS-I spacecraft enter the earth's atmosphere. The instrumentation on board the balloon payloads consisted of high time resolution (better than that attainable with the electron spectrometer) x-ray detectors sensitive to x-rays in the range 20-50 keV and above 50 keV. Cross correlation of the balloon data with data taken simultaneously by the spectrometer on ATS-I illuminated the nature of the electron acceleration and precipitation processes. Since the satellite is relatively stationary with respect to the earth's magnetic field lines, it is possible to obtain long periods (on the order of hours) of data taken by both balloon payloads and the spectrometer in the vicinity of the same field lines.

(4) Maximum Time Resolution Plots: Some of the data from the low energy channel was plotted with maximum time resolution as a function of time in an effort to see microbursts of electrons and/or other phenomena which have a time scale on the order of a few seconds to a few minutes. (Figure (4) is an example of such a plot.)

IV. Achievements

Several papers have been published in the scientific journals discussing both the general aspects and the unique events measured and analyzed through the course of this experiment. In addition, Monthly and Quarterly Data Reports were submitted compiling the pertinent details of the recovered data. Abstracts of the key papers are presented here to provide a brief overview of the results.

A. Abstracts of Reported Results

(1) Measurement and Intensity of Energetic Electrons at the Equator at 6.6 R_e

T.W. Lezniak, R.L. Arnoldy, G.K. Parks, and J.R. Winckler
School of Physics and Astronomy, University of Minnesota

RADIO SCIENCE, Vol. 3 (New Series), No. 7, July, 1968 p. 710

This paper presents preliminary results of measurements of 50 to 1000 keV electrons at the geomagnetic equator at 6.6 R_e. Quiet-day electron fluxes exhibit a diurnal dip in intensity at local midnight accompanied by a softening of the electron spectrum. During geomagnetically disturbed times the 50 to 150 keV electrons exhibit large fluctuations in intensity; we have denoted these fluctuations as "spikes." These spikes are largest just after local midnight and decrease in intensity as local time increases. They have a duration of about 1 hr and tend to recur with about a 2-hr period. The electron spectrum softens considerable during the spikes. Generally the variations in intensity of the electrons correlates excellently with the K_p index.

(2) Correlated Effects of Energetic Electrons at the 6.6 R_e Equator and the Auroral Zone During Magnetospheric Substorms

G.K. Parks, R.L. Arnoldy, T.W. Lezniak, and J.R. Winckler

School of Physics and Astronomy, University of Minnesota

RADIO SCIENCE, Vol. 3 (New Series) No. 7, July, 1968 p. 715

During magnetically disturbed times, large intensity variations are observed for electrons of energies 50- to 150 keV at the geostationary orbit of the ATS-I satellite. Simultaneously, the correlation experiment at the magnetic conjugate region of the satellite has shown that large fluxes of bremsstrahlung x-rays from precipitated energetic electrons are observed on high-altitude balloons while magnetic bays are recorded on the ground. The conclusion reached is that the magnetospheric substorm is responsible for the simultaneous intensification of the trapped particle population at 6.6 R_e equatorial plane and of precipitated energetic electrons at the magnetic conjugate region.

(3) Structure of the Magnetopause at 6.6 R_e in Terms of 50- to 150 keV Electrons

T. W. Lezniak and J. R. Winckler

School of Physics and Astronomy, University of Minnesota

Journal of Geophysical Research, Space Physics, Vol. 73, No. 17, Sept. 1, 1968
pp. 5733-5742

Measurements were made with a magnetic deflection electron spectrometer of electrons in the range 50-150 keV at the boundary of the magnetosphere on January 14, 1967. At this time, the magnetopause was compressed inside the orbit of the ATS-I geostationary satellite, which was located at 6.6 R_e in the sub-solar region of the magnetosphere. The first crossing of the trapping boundary and magnetic field reversal was followed by many transient count rate increases and magnetic field variations. Owing to the rapid sampling of electrons on the spinning satellite it was possible to determine the azimuthal distribution associated with electron concentration gradients at the various boundaries and to determine the direction in space of the gradients and of the trapping boundary surfaces. In one case the trapping boundary was found to be approximately perpendicular to the earth's surface. In another case a transient region was found that appeared to be moving over the spacecraft from the solar direction. The energetic electron trapping boundary was usually separated from the magnetic field reversal by the order of four cyclotron radii. The electron flux dropped from 1.4×10^4 to 3.2×10^2 (electrons cm^{-2} sec^{-1} $ster^{-1}$ keV^{-1}) in two cyclotron radii at one of these boundaries.

(4) Acceleration of Energetic Electrons Observed at the Synchronous Altitude During Magnetospheric Substorms

G. K. Parks and J. R. Winckler

Journal of Geophysical Research, Space Physics, Vol. 73, No. 17, Sept. 1, 1968
pp. 5786-5791

Correlation studies have been made between energetic electrons in three energy ranges: 50-150, 150-500, and 500-1000 keV measured at synchronous orbit and bremsstrahlung x-rays measured by balloons near the northern magnetic conjugate region increases in trapped electron fluxes are operated in close correlation with magnetospheric substorms as shown by magnetic bays in the auroral zone. These increases are always accompanied by an x-ray increase measured by the balloons with time profiles during the two hour substorm period correlating increase delayed even for 5 to 10 second pulsating structures. A dynamic Fourier Analysis indicates a predominant peak of the power spectrum at 2.5 hours. It is proposed that the substorm acceleration of these electrons provides an injection process for the outer radiation belt.

(5) Experimental Verification of Drift Shell Splitting in the Distorted Magnetosphere

K. A. Pfitzer, T. W. Lezniak, and J. R. Winckler

Journal of Geophysical Research, Space Physics, Vol. 74, No. 19, Sept. 1, 1969 pp. 4687-4693

School of Physics and Astronomy, University of Minnesota

Data from an electron spectrometer on the synchronous orbit satellite ATS-I and data from an electron spectrometer and ion chamber on the elliptical orbit satellite OGO-III can be used to experimentally test drift shell splitting in the non-dipolar distorted magnetosphere as proposed by Roederer. Quiet day pitch angle distributions obtained by ATS-I at 6.6 R_e qualitatively confirm the shell splitting by showing that near noon the pitch angle distribution is nearly isotropic whereas near midnight the pitch angle distribution is peaked toward small angles (parallel to the field). Using the Mead model magnetic field for calculating the drift shells for electrons of pitch angle $\alpha = 65°$ and $\alpha = 90°$, as well as the measured pitch angle distribution and measured radial gradient for electrons at local noon, the pitch angle distribution can be calculated as a function of local time for the ATS-I orbit. The agreement between calculated and measured fluxes is satisfactory not only in predicting the proper noon to midnight asymmetry (25 to 1 for 500-1000 keV electron on February 15, 1967) but also in correctly predicting the pitch angle distribution as a function of local time (isotropic at noon but non-isotropic with a 3 to 1 ratio between $\alpha = 65°$ and $\alpha = 90°$ at midnight). However, in one case (15 February, 1967) an asymmetry is observed about local midnight with minimum count rate at 2200 LT, representing a departure from the symmetric Mead model.

(6) Intensity Correlations and Substorm Electron Drift Effects in the Outer Radiation Belt Measured with the OGO-III and ATS-I Satellites

K. A. Pfitzer and J. R. Winckler

Journal of Geophysical Research, Vol. 74, No. 21, October 1, 1969, Technical Report CR-136, April, 1969

School of Physics and Astronomy, University of Minnesota

During late December 1966 and January 1967 the elliptically orbiting satellite OGO-III entered the magnetosphere within 30° of the subsolar point and within 10° of the geomagnetic equator. This permits the measurement of r_b, the distance to the magnetosphere boundary, which is a necessary parameter for the Mead model magnetic field calculations. The electron fluxes measured by an electron spectrometer and an ion chamber on OGO-III are correlated with electron fluxes on the geostationary satellite ATS-I at the exact time when both satellites are on the same drift shells as calculated from the Mead model magnetic field with separations in local time up to 180°. During quiet times an absolute comparison of the fluxes from 50-1000 keV gives a linear relationship indicating agreement of the measurements over a three order of magnitude range of intensities. During substorm increases the ATS-I measurements have similar profiles but are delayed in time with respect to each other. The observed delays are smaller for higher energy electrons and larger for greater separations in local time. As an example, the measured delays for 50, 150 and 400 keV electrons on January 11, 1967 when the local time separation was 110 are 26, 13-17 and 5 minutes, respectively. The observed delays are consistent with newly created electrons being produced in a region near local midnight. These newly produced electrons then gradient drift past the two satellites. The production region is shown to be 30°-60° in width and about 4 earth radii in depth.

(7) Simultaneous Observations of 5- to 15- Second Period Modulated Energetic Electron Fluxes at the Synchronous Altitude and the Auroral Zone

G. K. Parks and J. R. Winckler

School of Physics and Astronomy, University of Minnesota

Journal of Geophysical Research, Space Physics, Vol. 74, No. 16, August 1, 1969
pp. 4003-4017

Two magnetospheric substorm particle events recorded simultaneously at the 6.6 R_e equatorial plane and the conjugate region on earth in the auroral zone have been analyzed for fast temporal structures. The analysis indicates that the 10-second quasi-periodic modulations observed commonly in precipitation events also exist in trapped energetic electron fluxes confined in the equatorial plane. The Fourier spectral analysis shows a significant peak at 7-8 second periods for both the trapped and precipitated electron fluxes for the event shows a complicated multipeak frequency spectrum for both regions. The time development characteristics of these modulations are also studied by dynamic spectral analysis method. The coherence analysis of the two sets of data shows that the modulations in the equatorial plane and the auroral zone were generally uncorrelated, with the exception of a 6-minute duration at the beginning of the April 21, 1967, event. Finally, the analysis reveals that although the modulations in precipitated fluxes attained peak-to-valley flux ratios of about 2, the modulations in the equatorial plane were only a few per cent.

B. Studies and Conclusions Based on Results and Theoretical Interpretation

The primary purpose of this section is to interpret and summarize measurements on the injection and distribution of the energetic electron component of the trapped radiation as a result of magnetic storms. The results described herein have been obtained with magnetic deflection electron spectrometers carried in the OGO-I and OGO-III satellites in elliptical orbits penetrating both the inner and outer zone regions as well as the ATS-I geostationary orbit satellite in the outer zone, which is the subject of this report. Correlations with ground based magnetic and auroral measurements as well as high altitude balloons have played an important part in the interpretation of these results. The satellite instruments are similar on the various missions and details have been given in several papers and technical reports (see abstract section) also: (Lezniak et al., 1967, Pfitzer, 1968, Lezniak and Winckler, 1968, Pfitzer and Winckler, 1970.) The energy range extends from about 50 keV to several meV and it is possible to study the variation of the directional flux with pitch angle, with energy and with position in the trapping regions. The spectrometers on the OGO-I, OGO-III, and ATS-I satellites have now been directly compared in orbit at appropriate times and positions in the magnetosphere and agree to better than 10% using the laboratory calibration constants.

The most important single fact emerging from the ATS data is that the substorm, as a "subdivision" of magnetic storm activity, is directly associated with the injection of electrons into the outer zone. A significant observation was made by Brown, et al., (1968) who observed during the April 18, 1968 injection event mentioned earlier that electrons of E>300 keV were seen at intermediate L values (L=5.0) first at the exact time of a substorm near the beginning of this great magnetic storm event. Synchronous orbit observations and correlations between the ATS and OGO satellites have shown that the polar substorm as described by Akasofu (1968) plays a fundamental role in the injection,

modulation, and distribution of energetic particles in the radiation belts. The substorm associated variations observed during 24 hours at synchronous orbit are well shown by Figure 5, wherein is plotted appropriate ground based auroral zone magnetic records with local midnight indicated for each. Also is shown the three channels of the ATS spectrometer and the ATS total magnetic field furnished by Coleman and Cummings of U.C.L.A. The characteristic feature is the large increase seen in the electron fluxes at local midnight with the largest increase being associated with the low energy channel. The bay association of these increases at or shortly after midnight is well shown by the comparison with the College magnetometer. But even at other local times, one can plainly see by comparison with Leirvogur or Great Whale River records that fluctuations in the electron intensity are correlated with the bay event. Likewise, the spacecraft ambient magnetic field responds to these substorms. This correlation has been already discussed by Coleman and Cummings, (1968).

Insight into the nature of the outer zone variations has been gained by close comparison of the electrons fluxes measured by OGO-III and ATS-I. During the spring of 1967, OGO-III entered the noon side of the magnetosphere close to the equatorial plane and thus was in an ideal position to compare with the ATS-I satellite which revolved slowly over the 24-hour period at a constant radius of 6.6 R_e . It has been possible using the Roederer drift shell program to locate the electron drift shells in the distorted magnetosphere and to study the relationship of the quiet day and storm time changes seen on the two satellites (Pfitzer et al., 1969, Pfitzer and Winckler, 1969).

In Figure 6 is shown a quiet day comparison of the two satellites. The vertical line near the center marks the time when according to the computation the two satellites should be on the same drift shell. It is seen that at this time while the College magnetogram shows a quiet period the absolute fluxes of the two spectrometers agrees rather well. By contrast, in Figure 7 is shown a substorm increase in the lower energy channels of the two satellites

accompanying a bay disturbance at College. The substorm increase observed by the ATS-I satellite located at about 0300 local time heavy curve was also observed by the OGO-III satellite on the solar side of the magnetosphere but with an onset and general envelope delayed from that seen by ATS-I. The delay in onset is less for the high energy channel than for the low energy, also the rise of the electron increase is less steep as seen by OGO-III on the solar side then seen by ATS-I on the night side. We conclude that this observation shows the presence of a drifting group of electrons which are moving eastward in local time because of the gradient drift process in the magnetosphere. These electrons must have been injected near midnight at the time of the bay disturbance. Since this increase is typical of those seen on the ATS satellite as it remains almost stationary in the magnetic field in the outer zone, we conclude that such a substorm injection on the night side, followed by a drifting and smoothing effect, can populate the outer belt with electrons. Other examples of these correlations between the two satellites are shown in Figure 8 in schematic form. One sees that the satellite farthest from local midnight shows the smallest slope and the lowest maximum intensity. Also one notes that in one case, the two satellites were interchanged and in this case the OGO-III sees the event rise before the ATS satellite. A simple computer model has been applied to this situation and confirms quantitatively the delay times, rise times and energy dependencies of these substorm increases so they may with confidence be identified as injection events near local midnight followed by gradient drift in the nominal magnetosphere.

Similar evidence has been obtained by Arnoldy and Chan (1969) who have compared the time delay between the maximum of the simple bay disturbance seen at midnight with the maximum electron increase seen at synchronous orbit. They find that the delay increases uniformly with the local time as shown in Figure 9 (Midnight is at 10 UT for the ATS-I). This excellent correlation can be accounted for by drifting bunches of electrons of about 90 keV energy injected into the outer zone near midnight during a polar substorm.

Drift Shell Displacement and Magnetosphere Motion During Substorms

The substorm associated changes in the electron flux near midnight and through morning consists of large injection events for the 50 keV electrons accompanied by increases in other channels which may possibly be modulation as well as injection of fresh particles. But the behavior in the afternoon and evening sectors appears to be systematically different. In fact, an examination of various energy particles and their variations during substorms can give apparent clues as to the mode of motion of the magnetosphere during the substorm period. For this purpose the most energetic electrons are useful because their energy is affected least by the substorm and their drift period is very short compared to the substorm period of about two hours. Figure 10 shows a small substorm in the evening sector observed by the magnetometer at Fort Churchill which shows an almost identical modulation of all of the energy channels of the ATS and as well the total magnetic field. In fact, some of the features of the bay electrojet current are even reproduced in the electron variations. A notable exception is the presence in the low energy channel of two smooth increases delayed after the two main parts of the bay. These are almost certainly drifting bunches of electrons which were actually injected near local midnight, and have drifted around almost 24 hours in local time where they are observed in the evening sector. This bay disturbance evidently injected a double peak of low energy electrons. The correlation of the ATS measured magnetic field and the 500-1000 keV electron intensity is shown in Figure 11. To first order the particle and field values lie on a correlation curve during the substorm variation shown in the previous figure. We take this to be evidence for a motion of the electron drift shells over the stationary spacecraft due to an effective magnetospheric motion. During a substorm, this motion has the sense that the magnetosphere expands in the eventing sector with a weakening of the magnetic field and an inward motion of energetic particle drift shells. Investigation shows that at midnight the sense of the motion

suddenly reverses and during a substorm there is a collapse of the magnetosphere with an increase in the magnetic field and an outward motion of the drift shells. The evidence for this is presented in Figure 12. Here we show the correlation between the high energy electron channel and magnetic bay disturbances observed for stations near midnight but with the satellite either in the evening or in the postmidnight sector. It is seen that for bay disturbances when the satellite was in the evening sector the trend of the modulation is downward for the energetic electrons, while for bay disturbances when the satellite was in the postmidnight sector, the sense of the modulation is upward. One can thus visualize a type of fault line occurring approximately at midnight as shown in Figure 13 with the contours of constant $\underline{B}$ which would be followed by the electrons under ideal conditions shown displaced from their equilibrium position as they move during a substorm. This drift shell motion is consistent with the piling up of the lines of force in the postmidnight sector simultaneously accompanied by an expansion of the magnetic field in the evening. The situation referred to here would be typical of a region near the equatorial plane and near synchronous orbit.

The measurement of substorm effects on the trapped particles are complicated by the continually changing pitch angle viewed by the ATS instruments as the magnetic field tilts and distorts away from its quiet day configuration. There are very large effects on the pitch angle distribution during substorm or even during quiet days because of the drift shell splitting phenomena which occurs in the distorted magnetosphere. It has been possible to quantitatively evaluate the pitch angle distributions at different points in the magnetosphere by comparing the radial distribution measured by OGO-III with the pitch angle distribution measured at various local times by ATS-I (Pfitzer et al., 1969). The quiet day example in Figure 14 shows the typical large intensity of particles aligned along the field over the midnight region. By contrast in Figure 15, we see a similar range of pitch angles measured during a time of large substorm

activity on 8 February, 1967. The striking feature of this figure is that although in the evening and morning sectors, the tendency for the pitch angle distributions is to resemble those on a quiet day, near midnight during the large substorm increase the tendency is completely different and the pitch angle distributions become isotropic. It is believed that this isotropic behavior is consistent with the collapse or compression of the magnetosphere at that time away from the distorted condition so that it resembles more closely a circularly symmetric dipole type configuration in which drift shell splitting is absent. Thus this observation is consistent with the rapid compression during a substorm in the post-midnight region of the magnetic field. Figure 15 also gives indirect evidence for the injection of particles near midnight as one can see that the shell splitting gradually develops towards morning hours beginning with a condition of isotropicity near midnight.

The Acceleration of Electrons Near Midnight

Because of the availability of the vector magnetic field for many of the major magnetic storms seen by ATS-I, it is possible to construct a semi-quantitative picture of the midnight acceleration process. In Figure 16 is shown the substorms on 8 February with the total magnetic field and also the angle θ of inclination of the field to the polar axis. Typically during a substorm the magnetic field inflates and tips outward ($\theta > 11°$) in the dusk or pre-midnight local time quadrant. However, the field exhibits a sudden temporal collapse seen by the satellite provided it is within a small local time sector usually located within a few hours of local midnight. This collapse as described previously is accompanied by a magnetic bay disturbance at auroral stations also near local midnight and is therefore a universal time phenomenon and not a stationary pattern through which the satellite moves.

Because of the large values of θ observed in the vicinity of the spacecraft in the evening quadrant, these field lines may extend considerably beyond the synchronous orbit into the geomagnetic tail before returning to the earth.

As the collapse begins near midnight, these field lines snap inwards very rapidly (the convection velocity is estimated at 0.5 R_e/minute) bringing with them and heating in the process magnetotail plasma by means of the betatron and Fermi mechanisms (see Figure 17). The observed snapping of the field lines is sufficiently rapid that the convective velocity component for up to 20 keV particles is larger than the sum of the gradient and curvature drift components and the acceleration may continue for some time before the particles drift easterly out of the convection region. (For 5 keV particles, the sum of the longitudinal drift components is estimated at 0.11 and 0.039 R_e/minute at 12 and 7 R_e respectively, much less than the convective component 0.5 R_e/minute.) Since the magnetic field strength on a collapsing line may change tenfold, and since the length of a field line could decrease by a factor of three during the collapse, conservation of the first two adiabatic invariants predicts that particles could have their energies increased tenfold by this process.

One therefore views the injection of energetic electrons into the outer Van Allen belt as an impulsive, substorm-associated process. As the substorm develops there is an inward convective surge and simultaneous heating of magnetotail plasma as the post-midnight field lines collapse inward. The collapse begins near the synchronous orbit and progresses outward toward the tail as the substorm grows; this region of catastrophic collapse is (at least at synchronous orbit) less than 45° wide, and its westward edge is usually located just after local midnight. The particles receive their energy from the snapping in of distended, closed field lines--it is not necessary to postulate that field line annihilation is the particle energy source. As the particles convect inward and acquire more and more energy, the gradient and curvature drift velocity components gradually overpower the convective component and the particles longitudinally drift through the electric fields established by the gross magnetospheric motions. This produces further acceleration and

deceleration. Computations employing only the betatron mechanism and a typical electron differential energy spectrum at 17 R_e in the magnetotail reported by Bame et al., (1967) indicate that this mechanism can adequately account for the peak 50-150 keV electron flux observed at sychronous orbit during the midnight collapse.

The observations and ideas on which are based this picture of electron acceleration are well supported by previous experimental and theoretical work. Observations of increases in the outer zone energetic electron flux in correlation with magnetic bays have been observed by the Alouette satellite and reported by McDiarmid (1969). Rao (1969) has also described similar increases of energetic electrons closely correlated with bays on the basis of the polar orbiting Injun IV observations. Rao notes that the outer zone flux increases without a change in the trapping boundary latitude as the bay develops but with a poleward motion of the trapping boundary as a bay subsides.

The Alouette evidence is concerned with very large storms and shows that the source may extend well into the morning region. Gradient drift effects, however, may be present in the Alouette data which would localize the source more near the midnight meridian. A connection between electron islands seen in the earth's magnetic tail and substorms has been demonstrated by Rothwell and Wallington (1968), who conclude that the substorm effect on energetic electrons starts inside the magnetosphere on closed field lines and the energetic particles then propagate outwards into the tail region.

One notes that the observations at synchronous orbit are in general agreement with these data but, in addition, because of the slow motion of the ATS-I satellite through the sun-earth reference frame, time variations may be uniquely seen. The great asymmetry present between the midnight-morning sector and the evening sector in the production of energetic electrons is particularly well shown on the ATS data. Also the successive substorm increases seen everywhere in the ATS orbit which can be attributed to a source near midnight is another unique feature.

Theoretical descriptions particularly applicable to substorms have been given by Axford (1967) and Atkinson (1966). Axford suggests also the importance of the betatron and Fermi processes in collapsing field lines on the night side, following earlier ideas of Dungey (1961). Our conclusions are not in disagreement with most of these ideas but again the observations at synchronous orbit show that the nightside magnetic field collapse occurs near local midnight in a small local region. It seems possible that viscous friction discussed by many writers and suggested by Atkinson as a means of inflation of the field in the evening sector coupled with the co-rotation of the region up to at least 8 earth radii on the night side might set up the conditions for a substorm collapse of the field. It does not seem necessary to invoke magnetic line annihilation per se to energize the particles or even to induce the instability responsible for the substorm. However, observations from on limited region of space such as that covered by the ATS orbit may admittedly give an incomplete and somewhat biased point of view. One is impressed, however, by the fact that on quiet days the co-rotating magnetosphere on the night side is somehow able to inflate smoothly and recompress through morning without substorms and without gross instabilities. During the period when substorms are occurring the recompression as one rotates with the earth seems to take place unstably and the extended field lines rush inward near the midnight meridian at a certain instant labeled by the start of a bay disturbance. The co-rotational energy thus seems to play an essential role in driving the substorm process, coupled with the viscous extension of the tail field lines in a still closed region of the magnetosphere.

V. New Technology

No new technology items were uncovered in the design and development of the instrument for this experiment. Periodic reviews were held with the design team in attempts to identify any potential items associated with this contract.

VI. BIBLIOGRAPHY

Akasofu, S. I., 1968, Polar and Magnetospheric Substorms, D. Reidel, Dordrecht.

Arnoldy, R. L. and Chan, K. W., 1969, Preprint, U. of New Hampshire, to be published, Jour. Geo. Res.

Atkinson, G., 1966, Jour. Geo. Res. 71, 5157.

Axford, W. I., 1967, Aurora and Airglow, Reinhold, New York, 499.

Bame, S. J. Asbridge, J. R., Felthouser, H. W., Hones, E. W. and Strong, I. B., 1967, Jour. Geo. Res. 72, 113.

Beall, D. S., Bostrom, C. O. and Williams, D. J., 1967, Jour. Geo. Res., 72, 3403.

Dungey, J. W., 1961, Phys. Rev. Letters, 6, 47.

Hess, W. N., The Radiation Belt and Magnetosphere, Blaisdell Publishing Company, 1968.

Kane, S. R., Pfitzer, K. A., and Winckler, J. R., "The Construction Calibration and Operation of the University of Minnesota Experiments for OGO-I and OGO-III", Technical Report CR-87, September, 1966, School of Physics and Astronomy, University of Minnesota, Minneapolis, Minnesota.

Lezniak, T. W., Arnoldy, R. L., Parks, G. K., and Winckler, J. R., Conjugate Effects on Energetic Electrons between the Equator at 6.6 R_e and the Auroral Zone, Parts 1 & 2, Technical Report CR-103, 20 pp. June, 1967.

Lezniak, T. W., Arnoldy, R. L., Parks, G. K. and Winckler, J. R., 1967, Conjugate Point Symposium, Boulder, Colo., June 13-16, 1967, Radio Science 3, 715.

Lezniak, T. W. and Winckler, J. R., Magnetospheric Substorm Effects on Energetic Electrons in the Outer Van Allen Belt, University of Minnesota, Technical Report CR-137, April, 1969.

Lezniak, T. W., Arnoldy, R. L., Parks, G. K. and Winckler, J. R., Measurement and Intensity of Energetic Electrons at the Equator at 6.6 R_e, Radio Science 3, No. 7, 710-714, July, 1968.

Lezniak, T. W. and Winckler, J. R., The Structure of the Magnetopause at 6.6 R_e in Terms of 50-150 keV Electrons, Technical Report CR-113, 35 pp., September, 1967. Published in Jour. Geo. Res., 73, No. 17, 5733-5742, September 1, 1968.

Lezniak, T. W. and Winckler, J. R., 1968, Jour. Geo. Res. 73, 5733.

McDiarmid, I. B., Burrows, J. R. and Wilson, M. D., 1969, Jour. Geo. Res. 74, 1749.

Parks, G. K. and Winckler, J. R., Acceleration of Energetic Electrons Observed at the Synchronous Altitude during Magnetospheric Substorms, Technical Report CR-120, 14 pp., July, 1968. Published in Jour. Geo. Res. 73, No. 17, 5786-5791, September 1, 1968.

Parks, G. K., Arnoldy, R. L., Lezniak, T. W. and Winckler, J. R., Correlated Effects of Energetic Electrons at the 6.6 R_e Equator and the Auroral Zone During Magnetospheric Substorms, Radio Science 3, No. 7, 715-719, July, 1968.

Parks, G. K., Relation of Magnetospheric Acceleration and Precipitation in the Auroral Energetic Electrons, University of Minnesota Technical Report CR-138, April, 1969.

Parks, G. K. and Winckler, J. R., Simultaneous Observations of 5-15 Second Period Modulated Energetic Electron Fluxes at the Synchronous Altitude and the Auroral Zone, University Of Minnesota Technical Report CR-129, February, 1969. To be pub. in the Jour. of Geo. Res.

Pfitzer, K. A., 1968, Ph.D. Thesis, U. of Minnesota, Cosmic Ray Technical Report CR-123, August, 1968.

Pfitzer, K. A., Lezniak, T. W. and Winckler, J. R., Experimental Verification of Drift Shell Splitting in the Distorted Magnetosphere, University of Minnesota Technical Report CR-133, April, 1969. (To be published Jour. Geo. Res.).

Pfitzer, K. A. and Winckler, J. R., Intensity Correlations and Substorm Electron Drift Effects in the Outer Radiation Belt Measured with the OGO-III and ATS-1 Satellites, University of Minnesota Technical Report CR-136, April, 1969. (To be published Jour. Geo. Res.).

Pfitzer, K. A. and Winckler, J. R., 1968, Jour. Geo. Res. 73, 5792.

Pfitzer, K. A., Lezniak, T. W. and Winckler, J. R., 1969, Jour. Geo. Res., to be published.

Pfitzer, K. A. and Winckler, J. R., 1969, Jour. Geo. Res., to be published.

Pfitzer, K. A. and Winckler, J. R., 1970, to be published.

Rao, C. S. R., 1969, Jour. Geo. Res. 74, 794.

Rosen, L., Parks, G. K. and J. R. Winckler, Electron Precipitation Patterns and Their Relation to Substorm Increases in 50-150 keV Electrons at the Synchronous Orbit, U. of Minnesota Technical Report CR-139, April, 1969.

Rothwell, P. and Wallington, V., 1968, Planet Space Sci. 16, 1441.

Williams, D. J. and Smith, A. M., February, 1965, "Trapped Electron Intensities at High Latitudes at 1100 Kilometers," Jour. of Geo. Res., 70:3, pp. 541-556.

Winckler, J. R., Bhavsar, P. D. and Anderson, K. A., September, 1962, "A Study of the Precipitation of Energetic Electrons from the Geomagnetic Field during Magnetic Storms," Jour. of Geo. Res., 67:10, pp. 3713-3736.

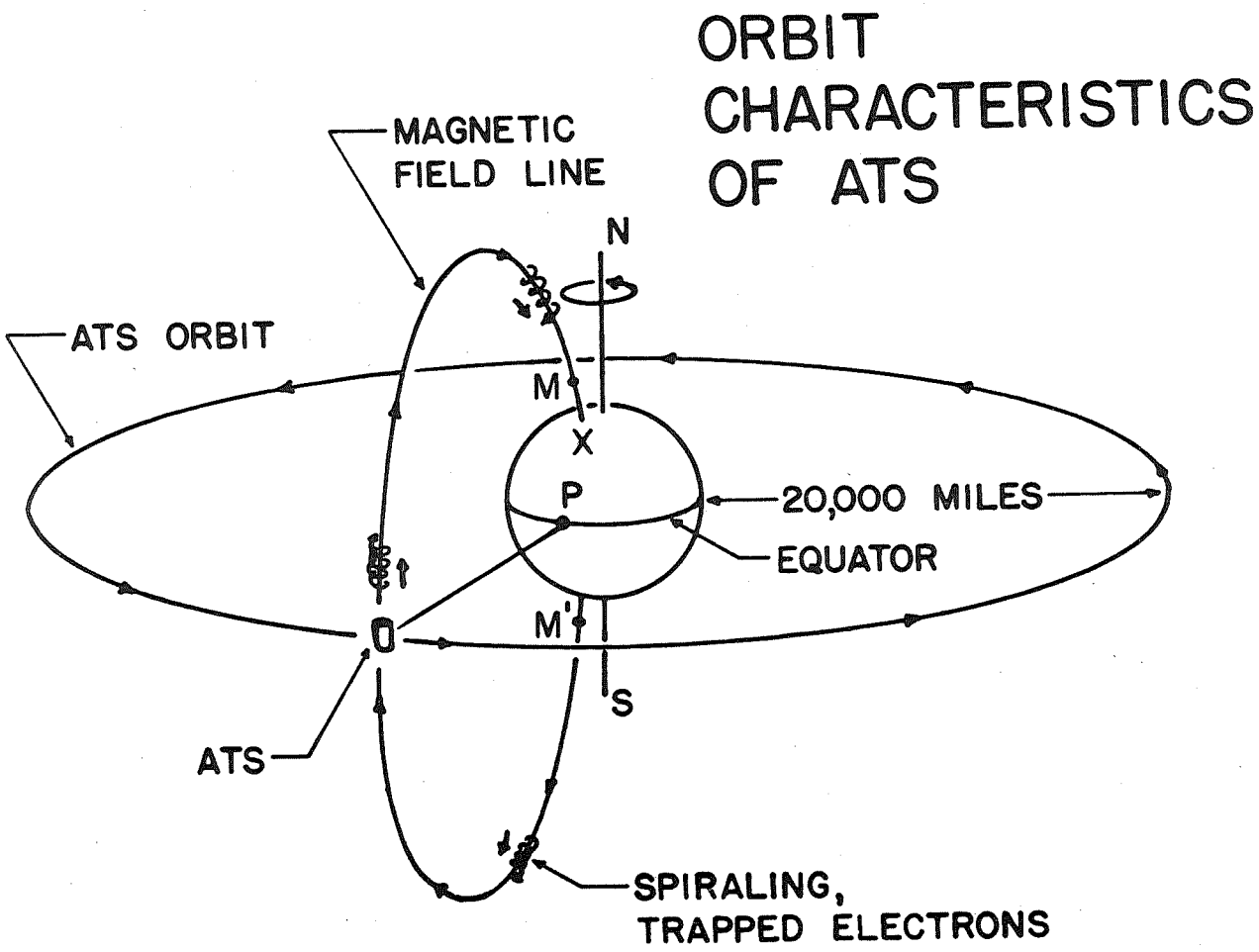
ORBIT
CHARACTERISTICS
OF ATS
MAGNETIC
FIELD LINE
N
ATS ORBIT
M
X
P
20,000 MILES
EQUATOR
M'
S
ATS
SPIRALING,
TRAPPED ELECTRONS

FIGURE 1

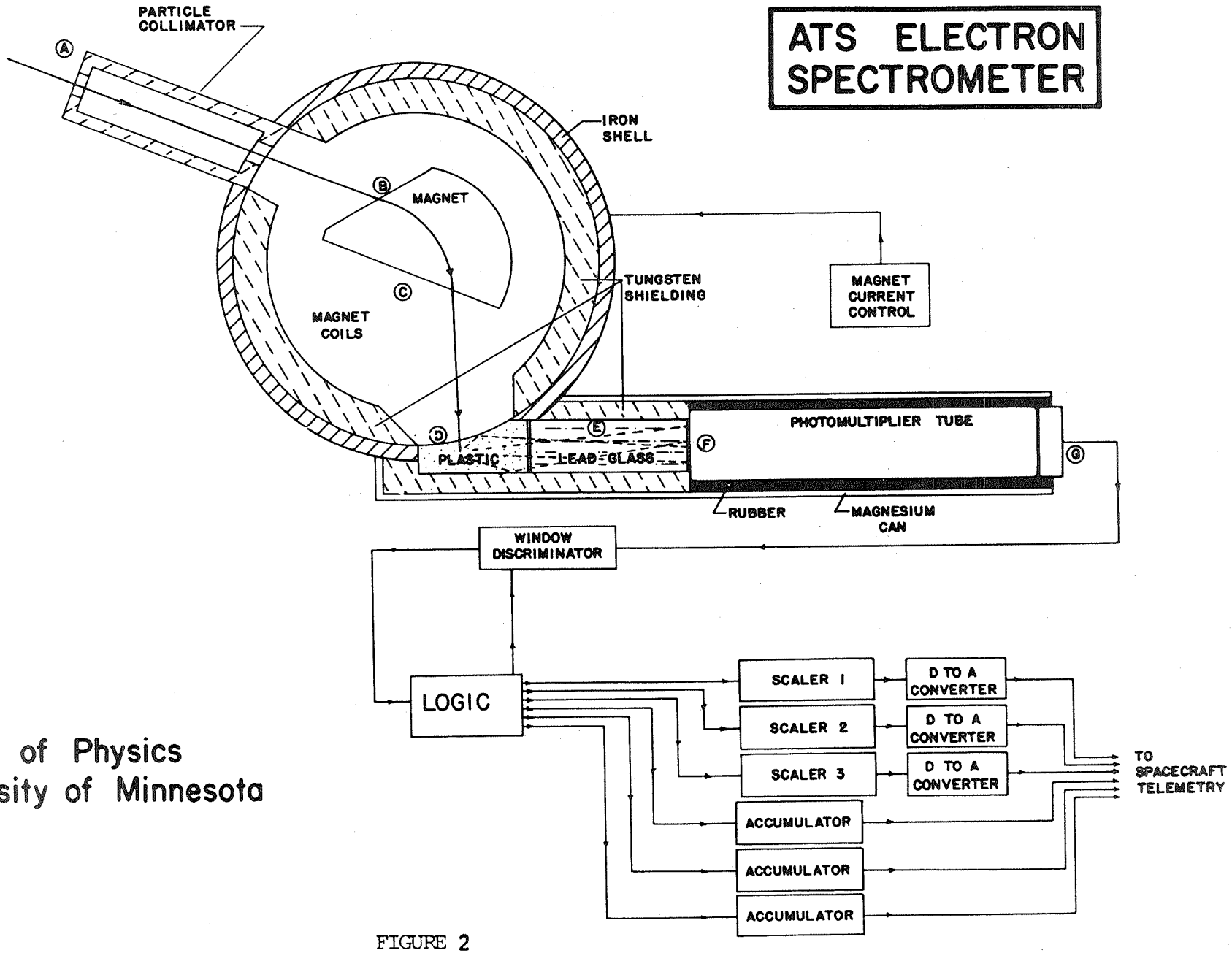

School of Physics
University of Minnesota

FIGURE 2

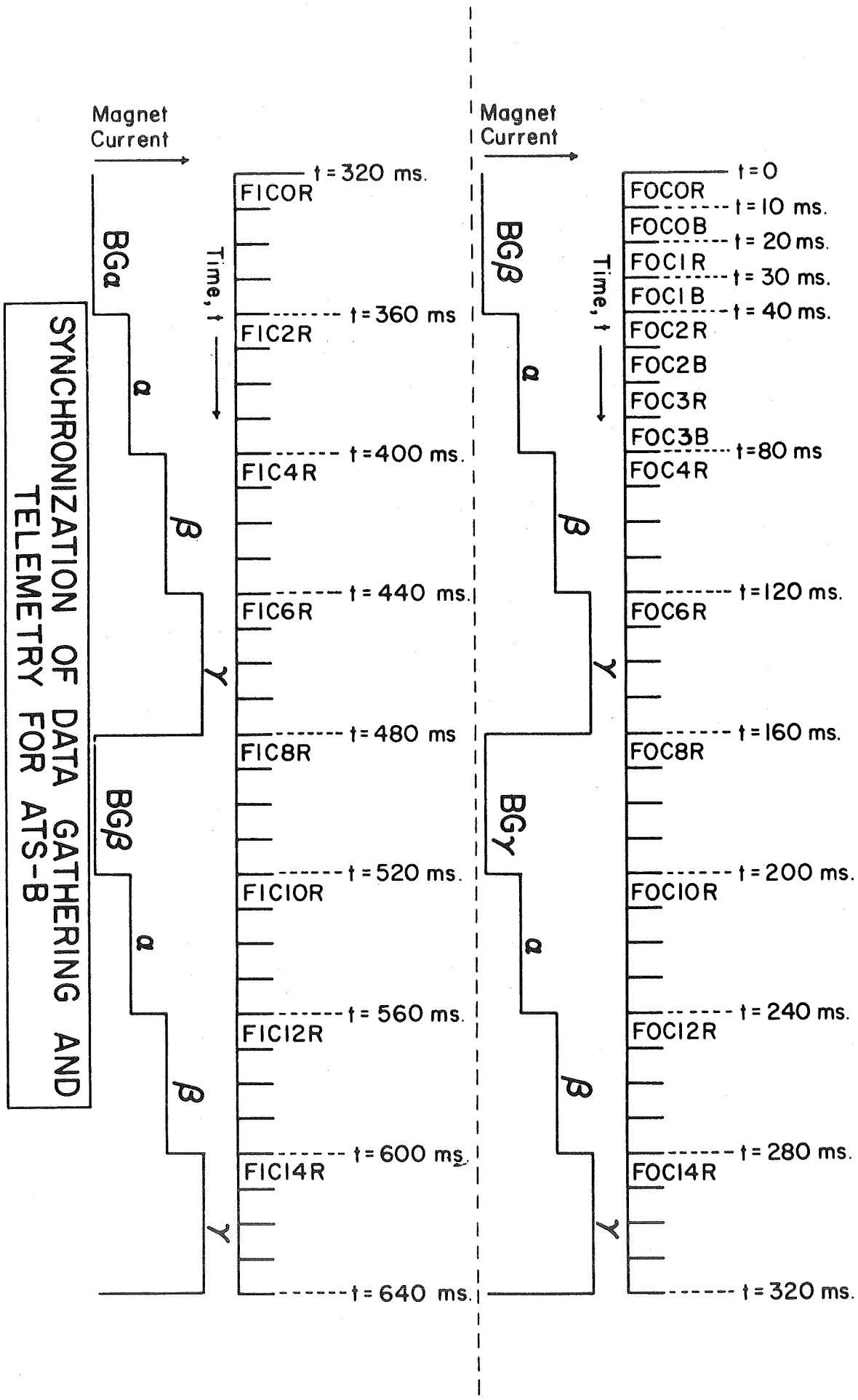
SYNCHRONIZATION OF DATA GATHERING AND TELEMETRY FOR ATS-B
Magnet Current
BGα
α
β
γ
BGβ
α
β
γ
Time, t
t = 320 ms.
FIC0R
t = 360 ms
FIC2R
t = 400 ms.
FIC4R
t = 440 ms.
FIC6R
t = 480 ms
FIC8R
t = 520 ms.
FIC10R
t = 560 ms.
FIC12R
t = 600 ms.
FIC14R
t = 640 ms.
Magnet Current
BGβ
α
β
γ
BGγ
α
β
γ
Time, t
t = 0
FOC0R
t = 10 ms.
FOC0B
t = 20 ms.
FOC1R
t = 30 ms.
FOC1B
t = 40 ms.
FOC2R
FOC2B
FOC3R
FOC3B
t = 80 ms
FOC4R
t = 120 ms.
FOC6R
t = 160 ms.
FOC8R
t = 200 ms.
FOC10R
t = 240 ms.
FOC12R
t = 280 ms.
FOC14R
t = 320 ms.

Figure 3

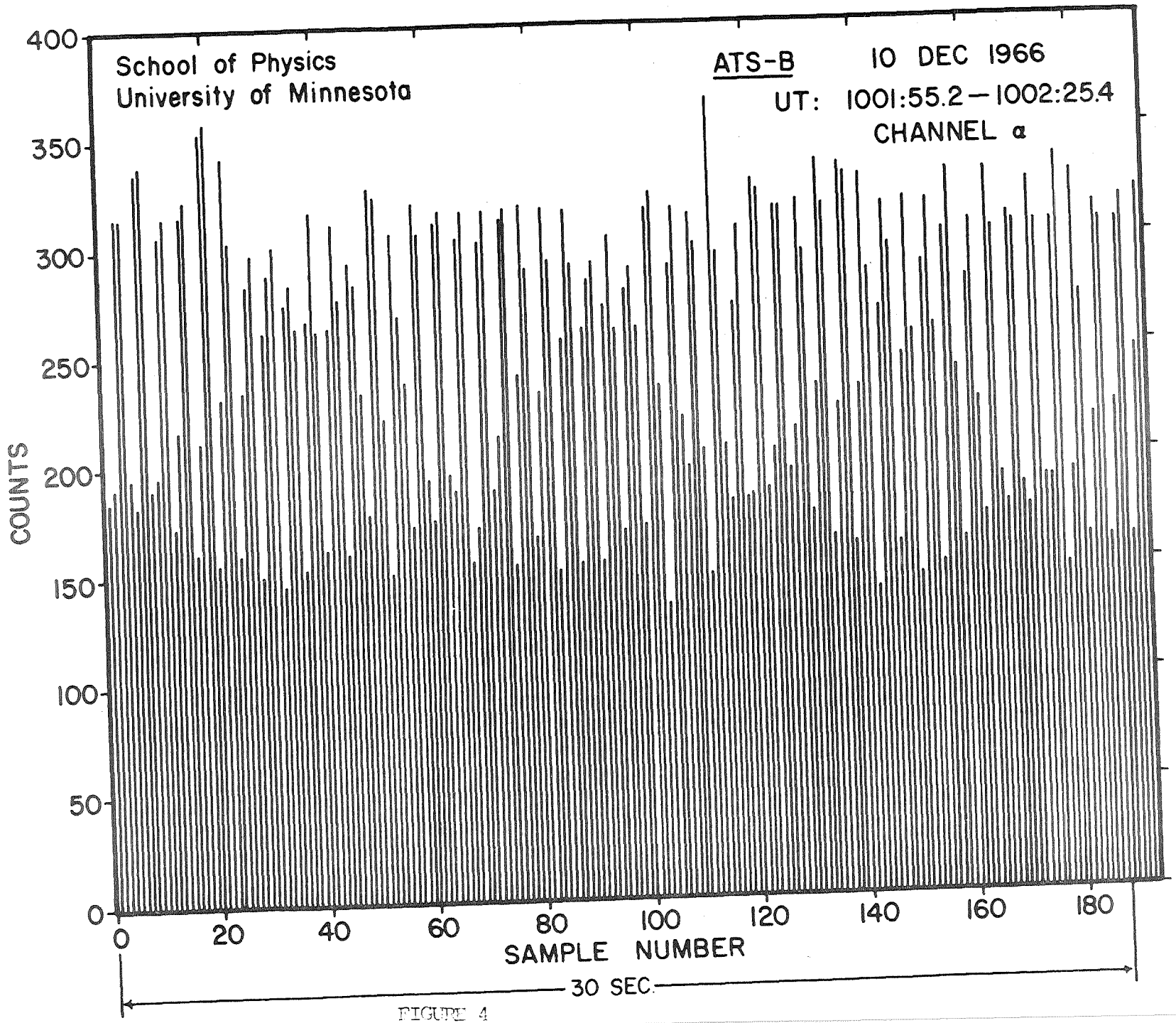
School of Physics
University of Minnesota
ATS-B
10 DEC 1966
UT: 1001:55.2 — 1002:25.4
CHANNEL α
COUNTS
400
350
300
250
200
150
100
50
0
0
20
40
60
80
100
120
140
160
180
SAMPLE NUMBER
30 SEC.

FIGURE 4

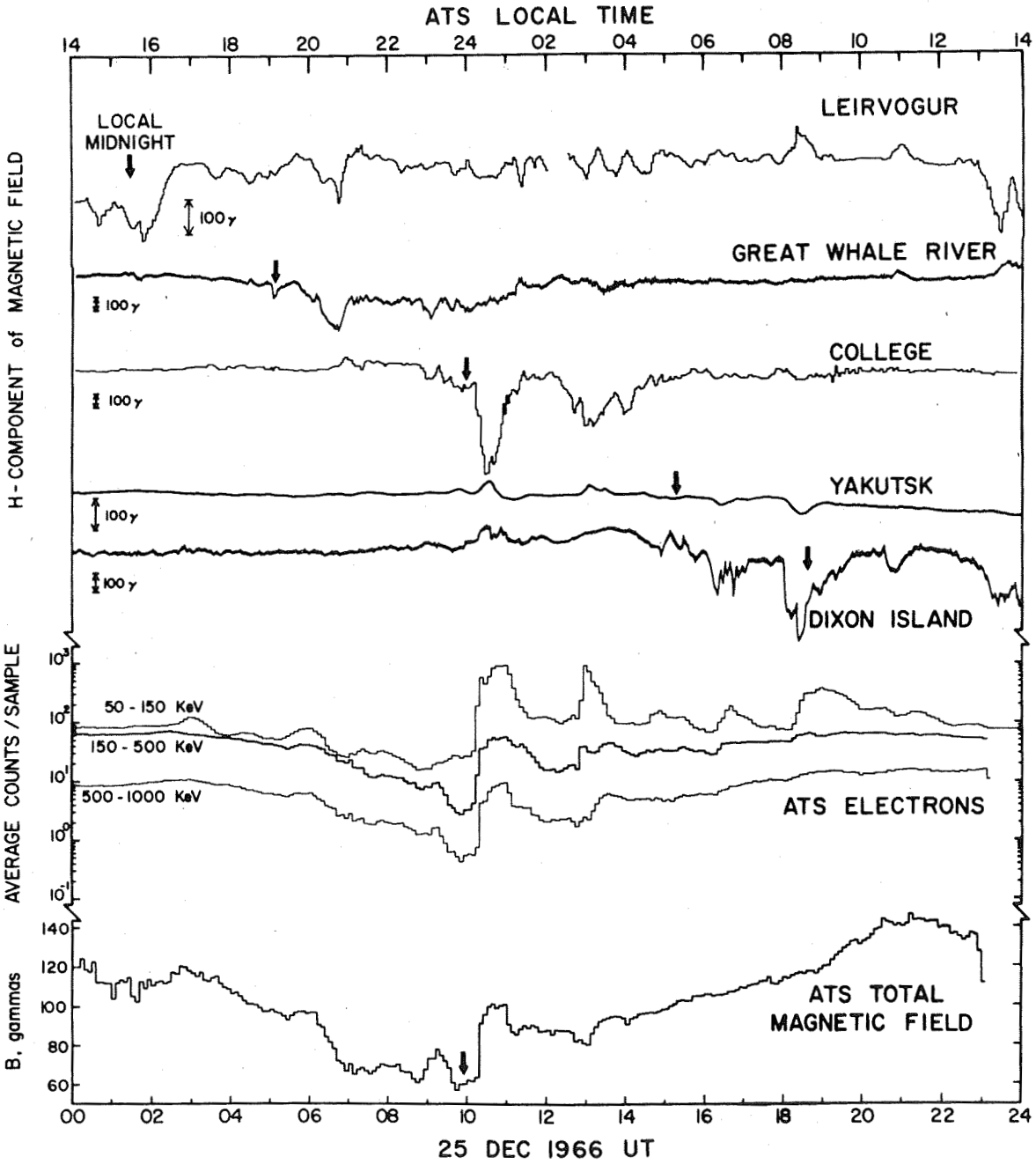
ATS LOCAL TIME
14 16 18 20 22 24 02 04 06 08 10 12 14
LOCAL MIDNIGHT
LEIRVOGUR
100γ
GREAT WHALE RIVER
100γ
COLLEGE
100γ
YAKUTSK
100γ
100γ
DIXON ISLAND
H-COMPONENT of MAGNETIC FIELD
AVERAGE COUNTS / SAMPLE
50 - 150 KeV
150 - 500 KeV
500 - 1000 KeV
ATS ELECTRONS
B, gammas
ATS TOTAL MAGNETIC FIELD
00 02 04 06 08 10 12 14 16 18 20 22 24
25 DEC 1966 UT

Figure 5

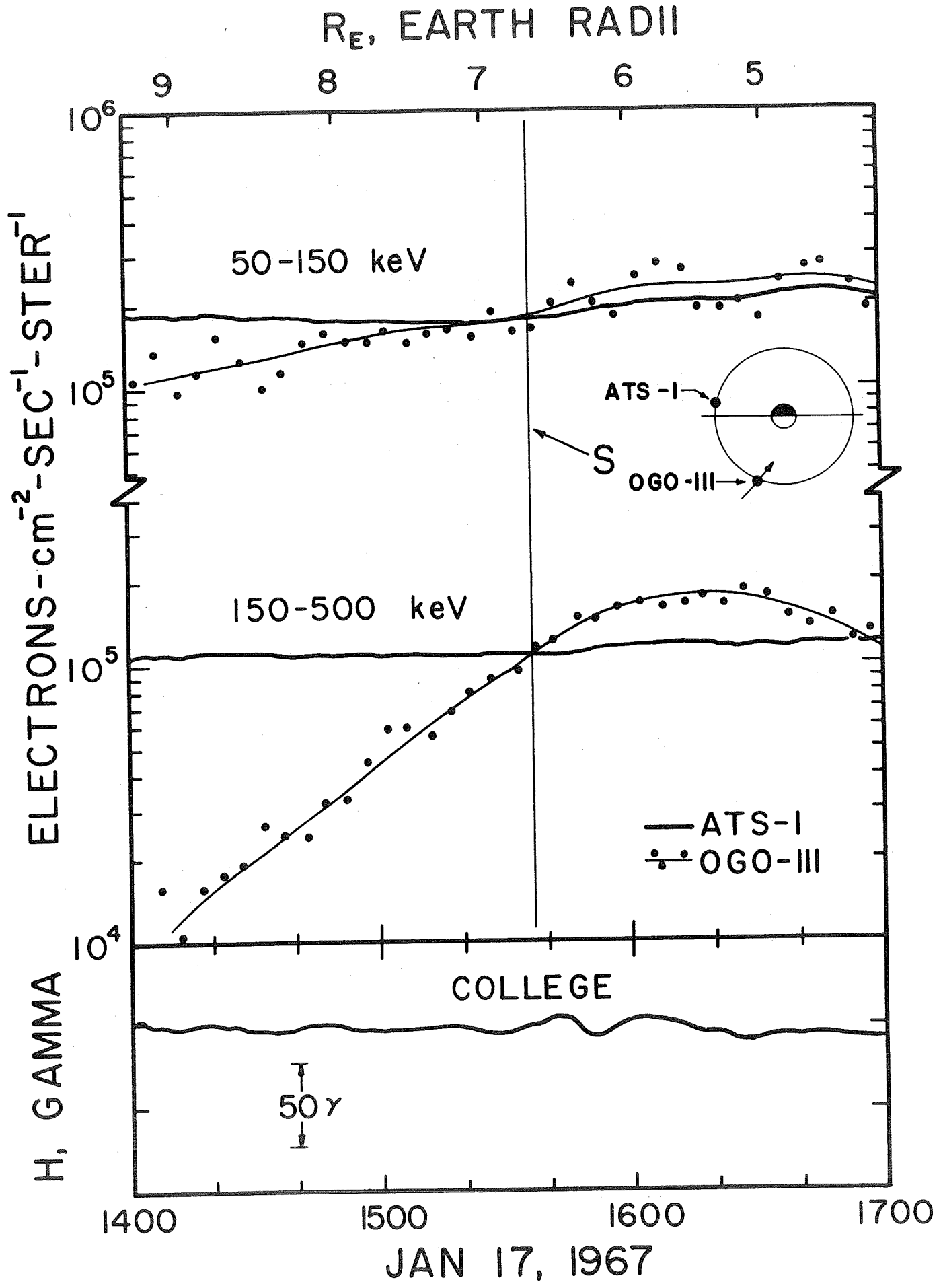
R_E, EARTH RADII
9
8
7
6
5
10^6
10^5
50-150 keV
ATS-I
S
OGO-III
150-500 keV
10^5
ELECTRONS-cm^-2-SEC^-1-STER^-1
—ATS-I
OGO-III
10^4
COLLEGE
50γ
H, GAMMA
1400
1500
1600
1700
JAN 17, 1967

Figure 6

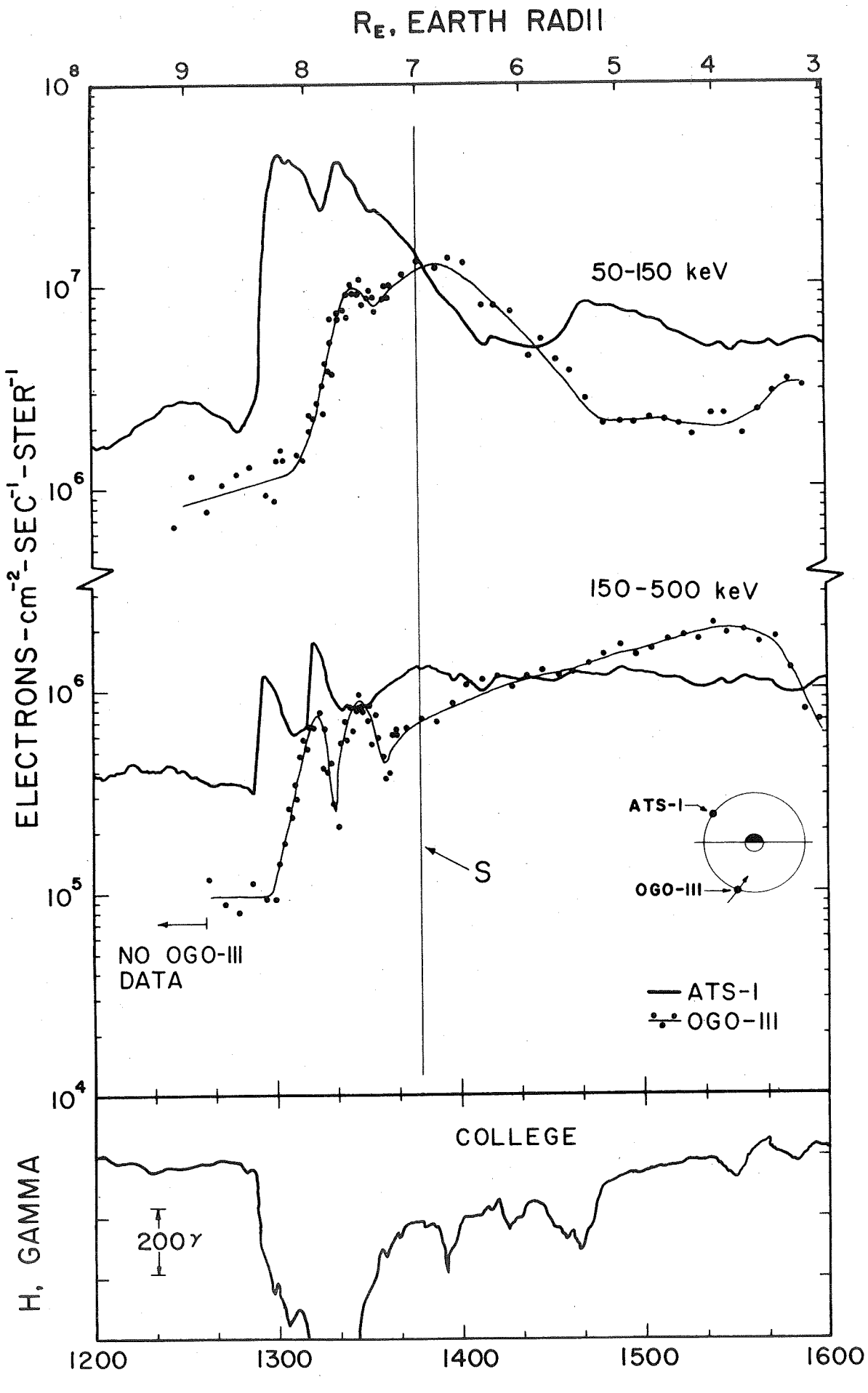
R_E, EARTH RADII
9
8
7
6
5
4
3
10^8
10^7
10^6
10^5
10^4
50-150 keV
150-500 keV
ELECTRONS-cm^{-2}-SEC^{-1}-STER^{-1}
ATS-I
OGO-III
S
NO OGO-III
DATA
ATS-I
OGO-III
COLLEGE
H, GAMMA
200γ
1200
1300
1400
1500
1600
JAN 11, 1967

Figure 7

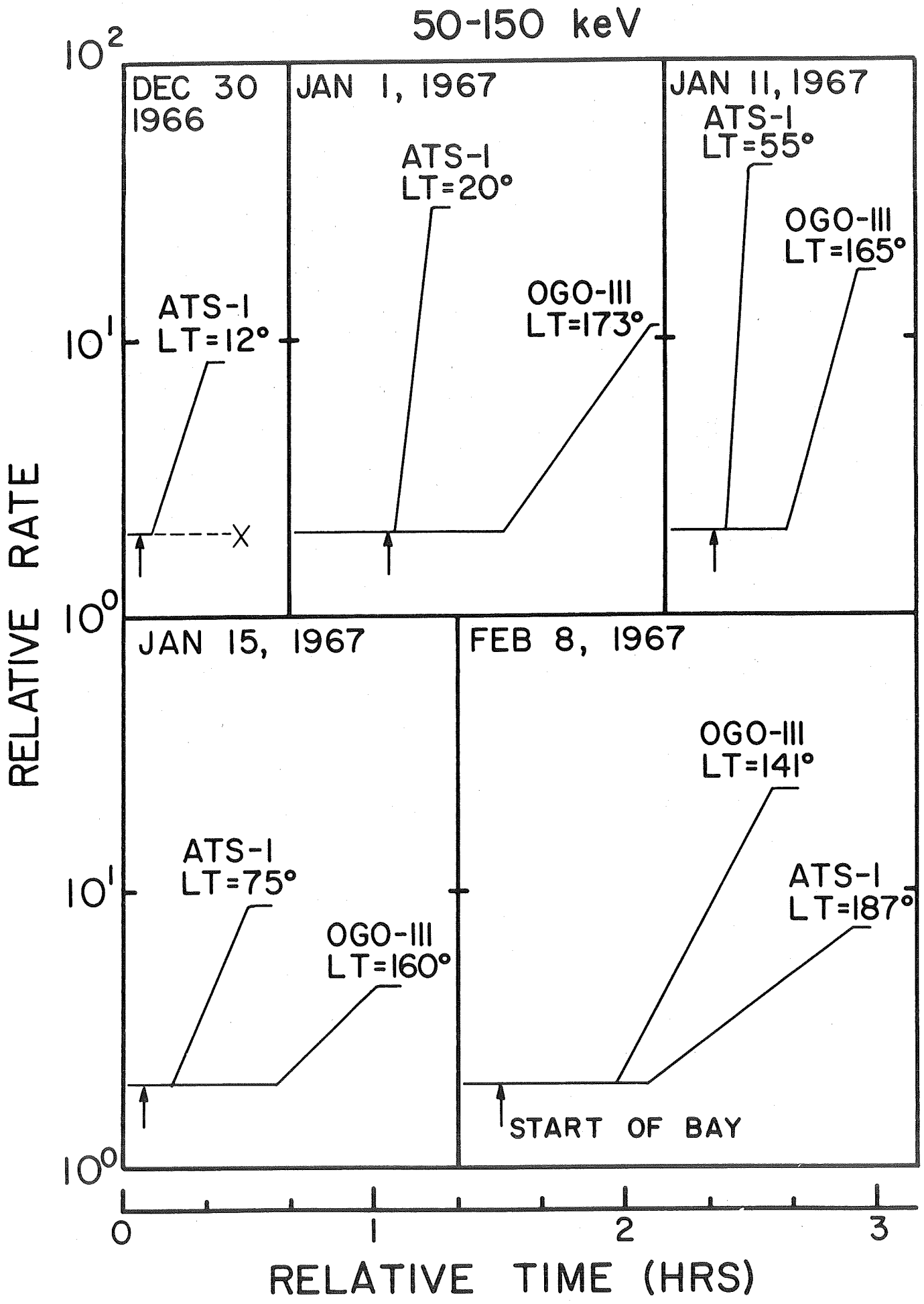
50-150 keV
DEC 30
1966
ATS-1
LT=12°
JAN 1, 1967
ATS-1
LT=20°
OGO-III
LT=173°
JAN 11, 1967
ATS-1
LT=55°
OGO-III
LT=165°
JAN 15, 1967
ATS-1
LT=75°
OGO-III
LT=160°
FEB 8, 1967
OGO-III
LT=141°
ATS-1
LT=187°
START OF BAY
RELATIVE RATE
RELATIVE TIME (HRS)

Figure 8

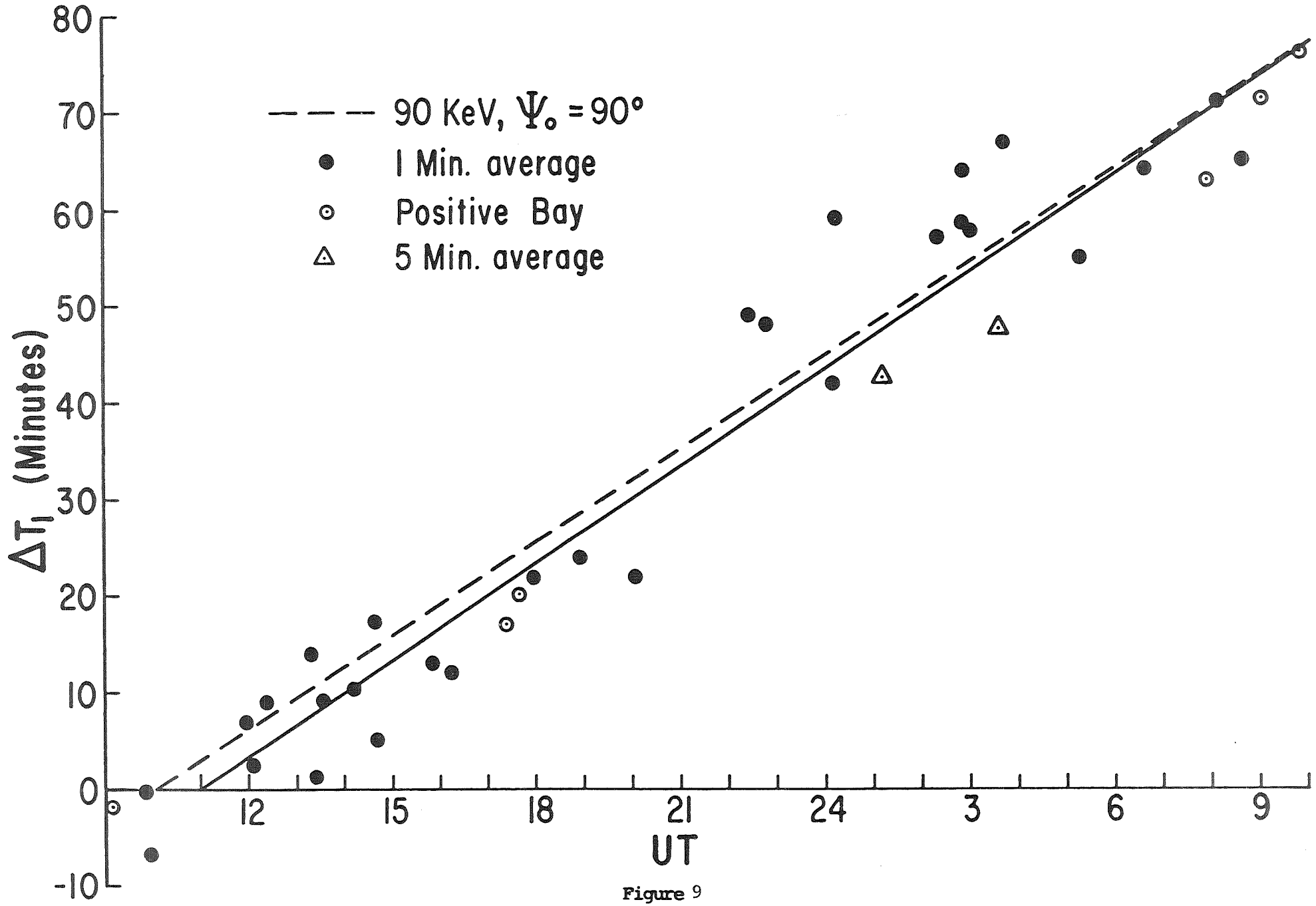
80
70
60
50
40
30
20
10
0
-10
ΔT_1 (Minutes)
90 KeV, $\Psi_o = 90°$
1 Min. average
Positive Bay
5 Min. average
12
15
18
21
24
3
6
9
UT

Figure 9

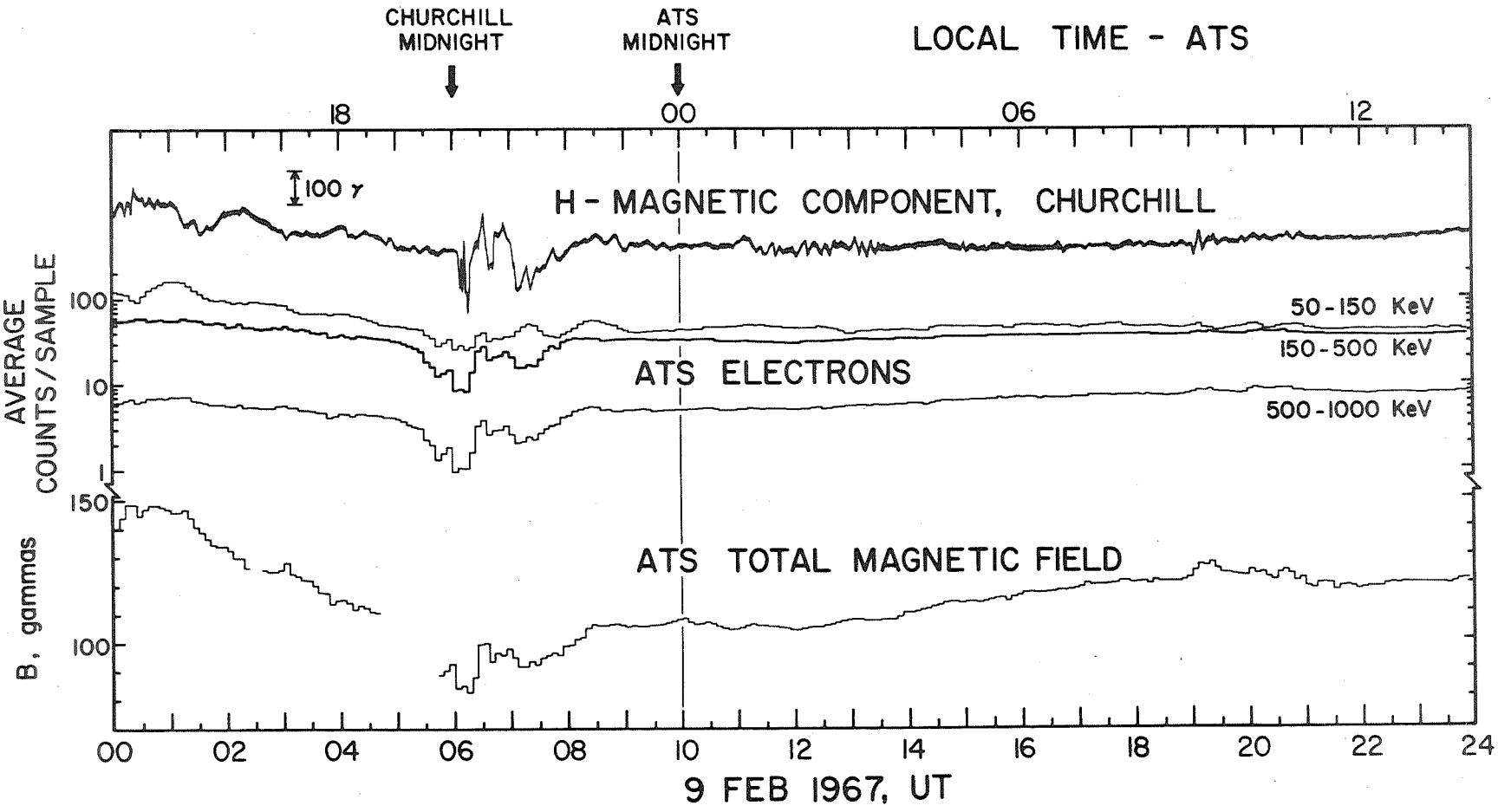
CHURCHILL MIDNIGHT
ATS MIDNIGHT
LOCAL TIME - ATS
18
00
06
12
100 γ
H - MAGNETIC COMPONENT, CHURCHILL
AVERAGE COUNTS/SAMPLE
100
10
50-150 KeV
150-500 KeV
ATS ELECTRONS
500-1000 KeV
150
B, gammas
ATS TOTAL MAGNETIC FIELD
100
00
02
04
06
08
10
12
14
16
18
20
22
24
9 FEB 1967, UT

Figure 10

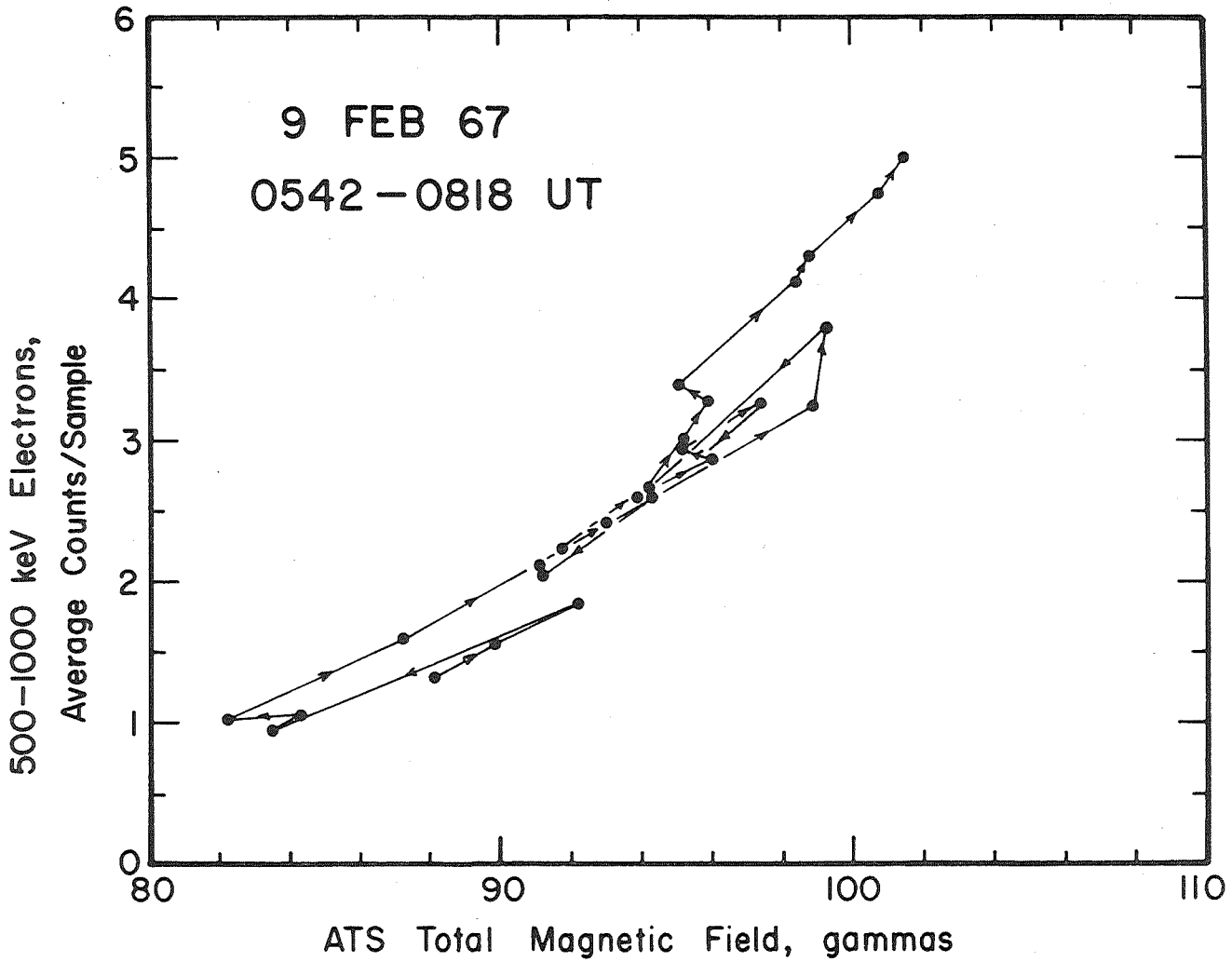
9 FEB 67
0542 – 0818 UT
500–1000 keV Electrons,
Average Counts/Sample
0
1
2
3
4
5
6
80
90
100
110
ATS Total Magnetic Field, gammas

Figure 11

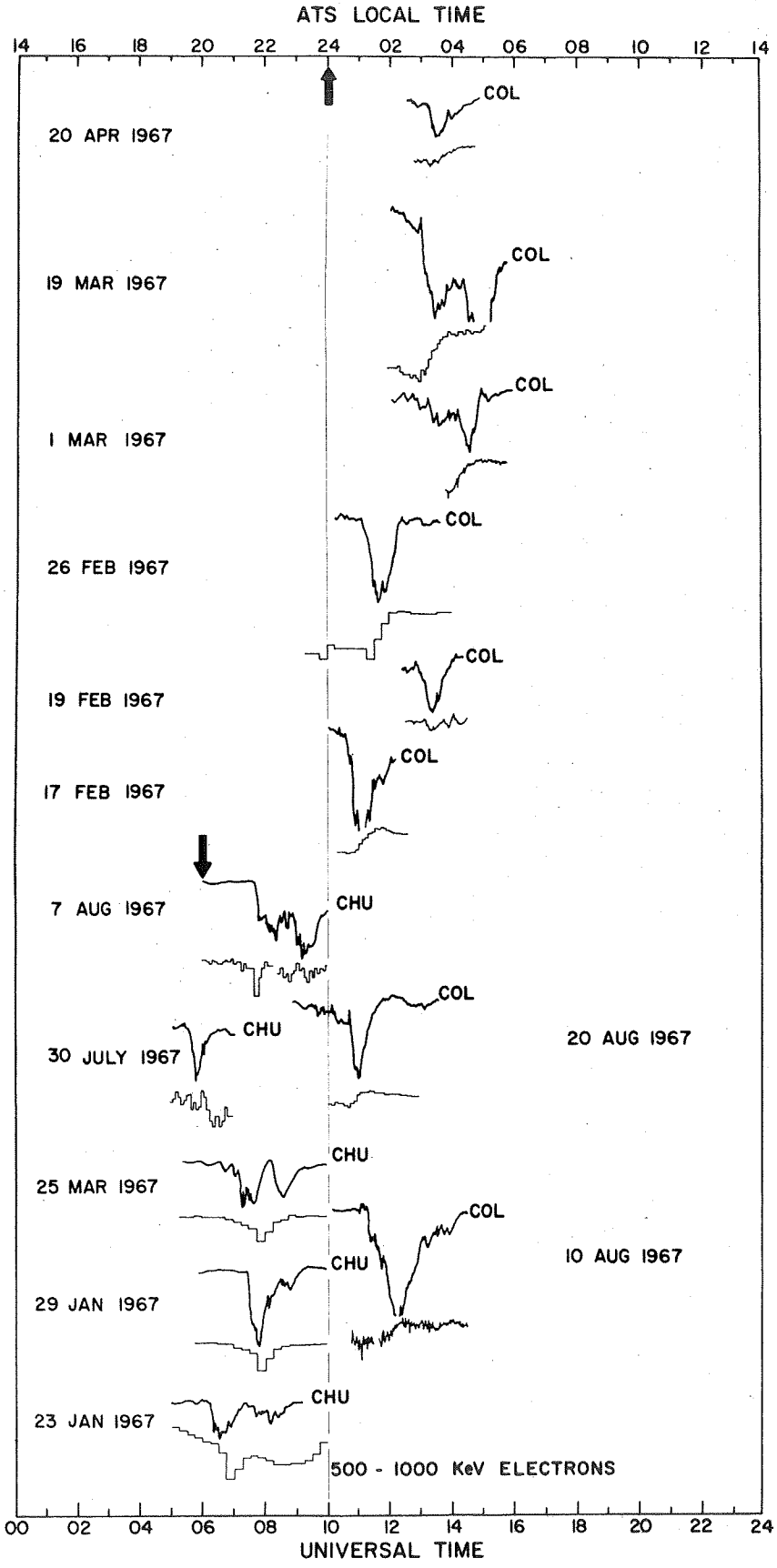
ATS LOCAL TIME
14 16 18 20 22 24 02 04 06 08 10 12 14
20 APR 1967
COL
19 MAR 1967
COL
1 MAR 1967
COL
26 FEB 1967
COL
19 FEB 1967
COL
17 FEB 1967
COL
7 AUG 1967
CHU
30 JULY 1967
CHU
COL
20 AUG 1967
25 MAR 1967
CHU
COL
10 AUG 1967
29 JAN 1967
CHU
23 JAN 1967
CHU
500 - 1000 KeV ELECTRONS
00 02 04 06 08 10 12 14 16 18 20 22 24
UNIVERSAL TIME

Figure 12

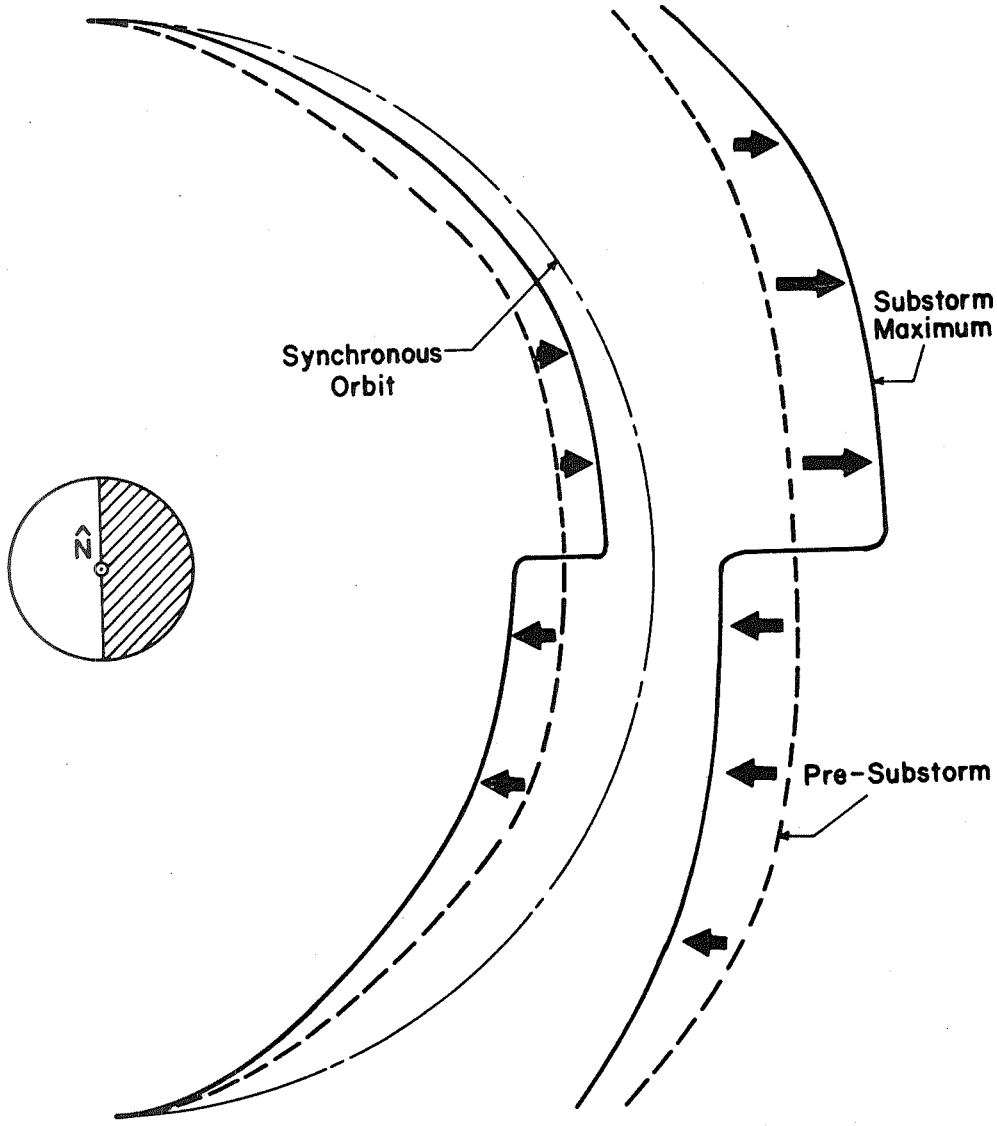

CONTOURS OF CONSTANT B IN THE EQUATORIAL PLANE

Figure 13

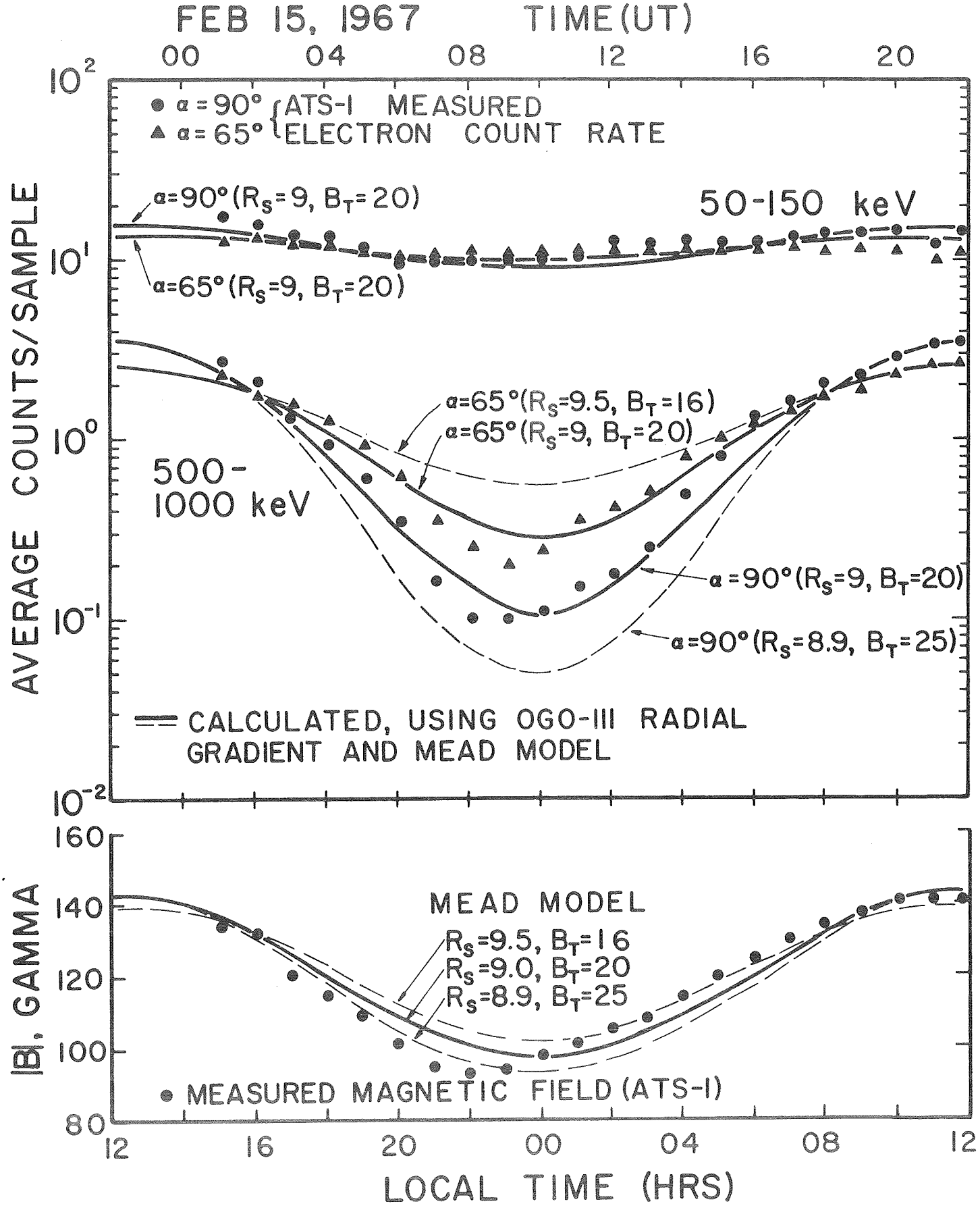
FEB 15, 1967 TIME(UT)
00 04 08 12 16 20
10^2
10^1
10^0
10^{-1}
10^{-2}
AVERAGE COUNTS/SAMPLE
● α = 90° } ATS-I MEASURED
▲ α = 65° } ELECTRON COUNT RATE
α=90° (R_S=9, B_T=20)
50-150 keV
α=65° (R_S=9, B_T=20)
α=65° (R_S=9.5, B_T=16)
α=65° (R_S=9, B_T=20)
500-
1000 keV
α=90° (R_S=9, B_T=20)
α=90° (R_S=8.9, B_T=25)
CALCULATED, USING OGO-III RADIAL
GRADIENT AND MEAD MODEL
160
140
120
100
80
|B|, GAMMA
MEAD MODEL
R_S=9.5, B_T=16
R_S=9.0, B_T=20
R_S=8.9, B_T=25
● MEASURED MAGNETIC FIELD (ATS-I)
12 16 20 00 04 08 12
LOCAL TIME (HRS)

Figure 14

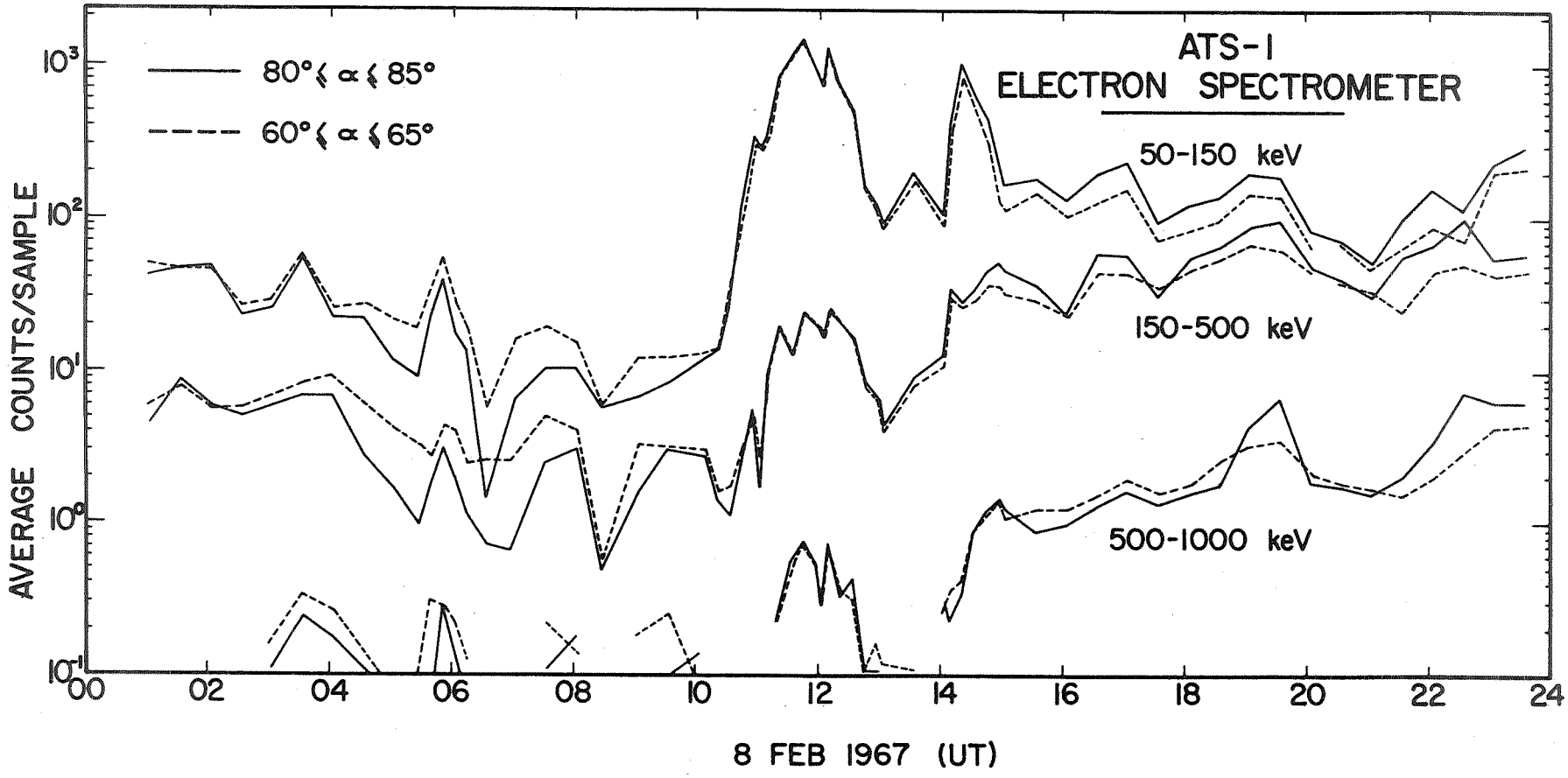
ATS-I
ELECTRON SPECTROMETER
80° ≤ α ≤ 85°
60° ≤ α ≤ 65°
50-150 keV
150-500 keV
500-1000 keV
AVERAGE COUNTS/SAMPLE
10³
10²
10¹
10⁰
10⁻¹
00
02
04
06
08
10
12
14
16
18
20
22
24
8 FEB 1967 (UT)

Figure 15

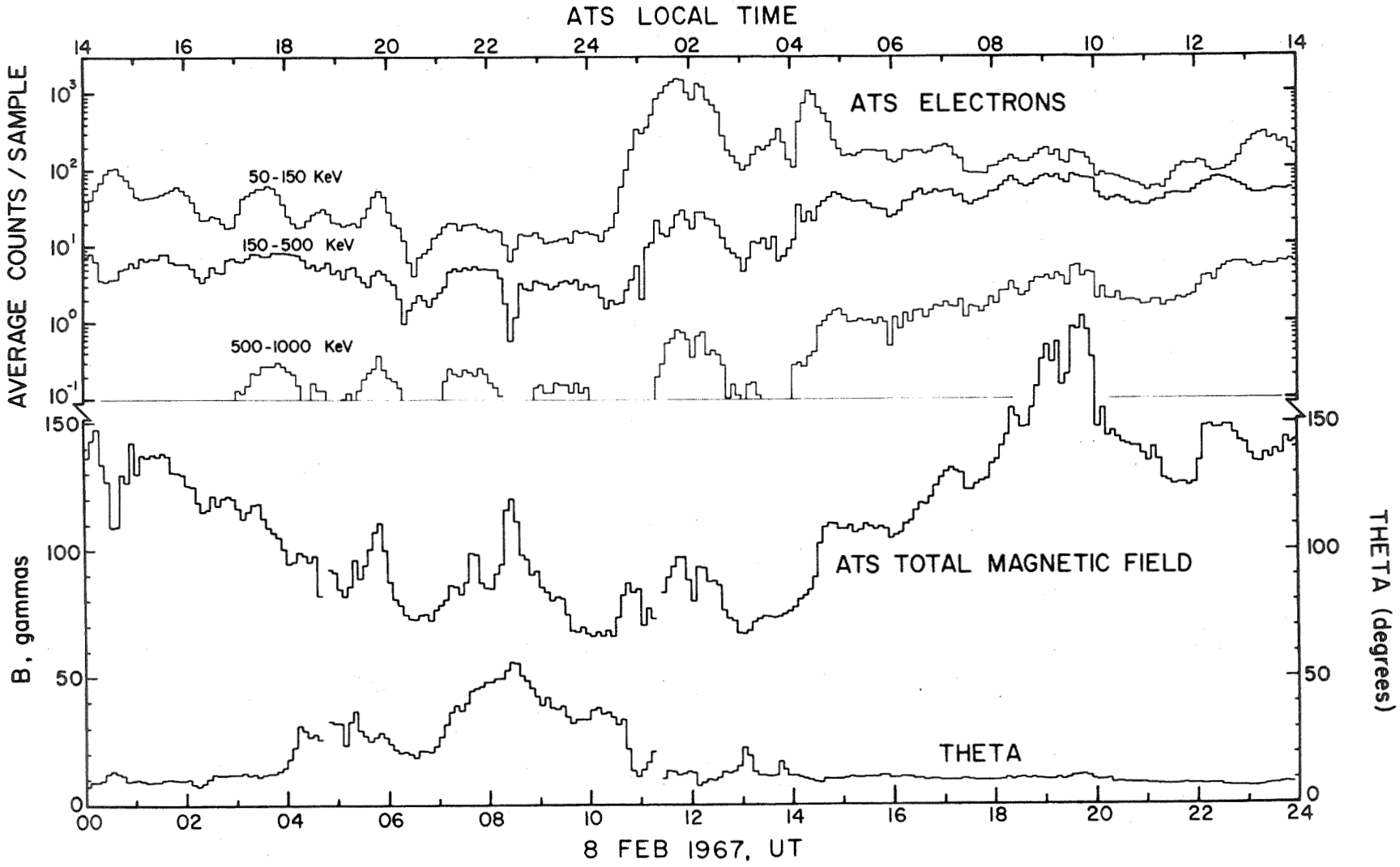
ATS LOCAL TIME
14 16 18 20 22 24 02 04 06 08 10 12 14
AVERAGE COUNTS / SAMPLE
ATS ELECTRONS
50-150 KeV
150-500 KeV
500-1000 KeV
B, gammas
ATS TOTAL MAGNETIC FIELD
THETA
THETA (degrees)
00 02 04 06 08 10 12 14 16 18 20 22 24
8 FEB 1967, UT

Figure 16

POST-MIDNIGHT COLLAPSE AND ACCELERATION

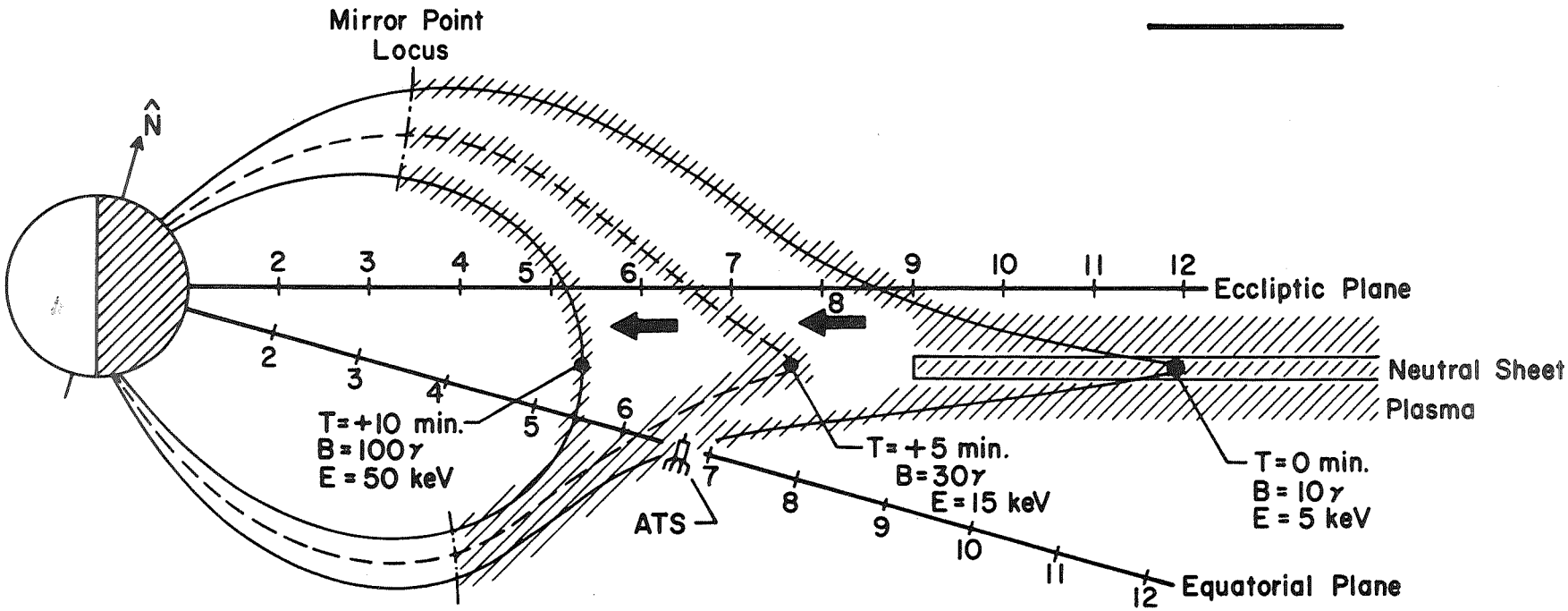

Figure 17